Chlorine as a substituent - from quantum chemistry and photoelectron spectroscopy

Maria Gundersen Zahl

Dissertation for the degree philosophiae doctor (PhD)
at the University of Bergen

2015

Dissertation date: February 17th

Soli Deo Gloria

You have made us for yourself, and our hearts are restless, until they can find rest in you.

Augustine of Hippo, in Confessions

Preface

The present thesis, submitted for the degree of philosophiae doctor at the University of Bergen, consists of a presentation of the methods and main results from five scientific papers. The work has been carried out at the Department of Chemistry under supervision of Leif J. Sæthre and Knut J. Børve from February 2007 until November 2014.

Two of the papers are a result of collaboration with Prof. Anne Borg, Trine H.-Andersen and Ingebor-Helene Svenum at Department of Physics at Norwegian University of Science and Technology, Trondheim. Also, we have had a close collaboration with Prof. T. Darrah Thomas at Oregon State University, Oregon.

Measurements were performed at the synchrotron facilities MAX-lab, Lund, Sweden and ALS, Berkeley, California.

This project was funded by the University of Bergen. The Norwegian Research Council has granted computational time through the Norwegian high-performance computer consortium (NOTUR).

Acknowledgments

First of all, I would like to sincerely thank my supervisors, Leif J. Sæthre and Knut J. Børve. I have had the privilege to be supervised by skilled and ambitious researchers who have been actively involved at every stage of the projects. Thank you for an open door and for always taking the time for me and my questions. Also, I am grateful for all of the practical care you have given me these years. I have indeed appreciated being one of your students. And behind every successful man... Tove and Kari Grete, I owe you a thank and an apologize for late working hours and delayed dinners.

T. Darrah Thomas, I am so glad that I was given the opportunity to work with you. It has been an honor and a pleasure - and great fun. Tom X. Carroll, you are thorough in all you do and always willing to offer your help. Thank you for all the interesting and fun hours of fellowship - both on and off duty. Other highlights have been meeting with colleagues from Trondheim and Uppsala, Trine H. Andersen, Svante Svensson and Henrik Bergersen.

During my time at the Department of Chemistry, I have enjoyed the company of numerous interesting and nice people that have encouraged me, each in their own way. In particular, I would like to thank Dorte, Anne, Mathias, Jarle, Velaug, Peng, Alf, Mahmoud, Randi, Nils, Karolina and Ingvild. Thank you, Elaine, for commenting on this thesis and even more for your friendship. To combine a PhD with family life has its challenges and I would like to thank the administration for providing flexible solutions and also for creating a positive working environment at the department. Alette and Randi - you are hospitality personified. Kristin, Karoline and Dora - I am so grateful for you.

I am in debt to my parents, for their support in so many ways. I also want to thank my parents-in-law. Thank you all for caring for me and my family through the years and not least at the last stage of this project.

Sverre, after ten years I am still convinced I could not have shared my life with anyone better than you. Ingrid, Elisabeth and Margrethe - you and dad make my life so beautiful and I am so grateful for all of you.

Bergen, November 2014
Maria Gundersen Zahl

Abstract

The role of chlorine as a substituent upon ionization, protonation and electrophilic addition of HCl has been studied by means of computational chemistry and photoelectron spectroscopy. Gas-phase carbon 1s photoelectron spectra of four chlorinated methanes (CCl_nH_{4-n}, n=1,2,3,4), six chlorinated ethenes ($C_2Cl_nH_{6-n}$) and seven chlorinated propenes are recorded. The spectra are analyzed by means of theoretical modeling and ionization energies for each inequivalent carbon are extracted. Furthermore, ground-state potentials for each site are computed and thereby the ionization energies can be decomposed into contributions from the ground state and relaxation, e.g. delocalization of charge in the final state. It is found that chlorine primarily acts by making the ground-state potential of the neighboring carbon more positive. However, upon ionization, chlorine also donates a significant amount of electrons both to a neighboring carbon and to a second-nearest π-bonded neighbor.

Activation energies for the electrophilic addition of HCl to the chlorinated ethenes and propenes are computed and probably we overestimate the energies by about 10% compared to experimental results. Protonation enthalpies are predicted with uncertainties of 0.09 eV or less. We find that chlorine upon protonation act as an effective electron donor via the π-system if in a neighboring position to the protonated carbon and that the effective donation is much larger for protonation than for ionization and electrophilic addition. The explanation is that the protonated site has an enhanced ability to accept electrons compared to if the same site is ionized or is subject to an electrophilic addition.

At room temperature, both 3-chloropropene and 2,3-dichloropropene possess two stable rotational conformers. As a part of the theoretical modeling of a spectrum, we predict a theoretical vibrational lineshape for each chemical inequivalent site in the molecule. As the theoretical lineshapes for each of these rotamers are qualitatively different, the relative intensities of the vibrational lineshapes could be optimized and thereby relative populations could be determined.

Adsorption of 1,1-dichloroethene ($Cl_2C{=}CH_2$) to a Si(111)-7×7 surface is studied by means of XPS. It is found that 1/3 of the molecules break one C-Cl bond and 2/3 break both C-Cl bonds when chemisorbing to the

surface. Physisorption spectra were compared to gas-phase spectra of the same compound, and it is found that except for broadening caused by the polarizable surface, the gas-phase spectrum constitutes an excellent model for the spectrum of the physisorbed species. We recommend that gas-phase spectra are used on a routine basis when assigning spectra of physisorbed species.

Comparing to experiments, we find that we are able to compute theoretical ionization energies within chemical accuracy, e.g. within 0.04 eV. However, our computed C-Cl bond lengths have deviations in the range of 0.6 pm whereas the desired accuracy is ± 0.1 pm. The inaccuracy is related to a very slow basis set convergence for chlorine, making it a demanding substituent to model.

Contents

List of publications

This dissertation is based on five scientific papers. The published papers are reprinted with permission from the publishers.

Paper [1]
Carbon 1s photoelectron lineshapes of the chlorinated methanes: Lifetimes and accurate vibrational lineshape models.
M. G. Zahl, K. J. Børve, and L. J. Sæthre.
J. Electron Spectrosc. Rel. Phenom., 2012, **185**, 226-233.

Paper [2]
Electronic Properties of Chlorine as Substituent to the Ethylenic Group - Viewed from the Core of Carbon.
M. G. Zahl, R. Fossheim, K. J. Børve, L. J. Sæthre, and T. D. Thomas.
In manuscript

Paper [3]
Proton Affinity as Predictor for Electrophilic Addition of HCl to Chlorinated Ethenes and Propenes A Critical Assessment.
M. G. Zahl, L. J. Sæthre, K. J. Børve, and T. D. Thomas.
In manuscript

Paper [4]
Chemisorption of 1,1-Dichloroethene on the Si(111)-7×7 Surface.
T. H. Andersen, M. G. Zahl, I.-H. Svenum, K. J. Børve, A. Borg, and L. J. Sæthre.
Surf. Sci., 2007, **601**, 5510-5514.

Paper [5]
Molecular Spectra As a Tool in Assigning Carbon 1s Photoelectron Spectra of Physisorbed Overlayers.
M. G. Zahl, V. Myrseth, T. H. Andersen, J. Harnes, A. Borg, L. J. Sæthre, and K. J. Børve.
J. Phys. Chem. C, 2010, **114**, 15383-15393.

In addition, I have contributed to the following publications although not included in this thesis:

Laboratory-frame electron angular distributions: Probing the chemical environment through intramolecular electron scattering.
M. Patanen, O. Travnikova, M. G. Zahl, J. Söderström, P. Decleva, T. D. Thomas, S. Svensson, N. Mårtensson, K. J. Børve, L. J. Sæthre, and C. Miron.
Physical Review A, 2013, **87**, 063420. [6]

Intensity oscillations in the carbon 1s ionization cross sections of 2-butyne.
T. X. Carroll, M. G. Zahl, K. J. Børve, L. J. Sæthre, P. Decleva, A. Ponzi, J. J. Kas, F. D. Vila, J. J. Rehr, and T. D. Thomas.
Journal of Chemical Physics, 2013, **138**, 234310,1-5. [7]

Comments on my own contributions

Paper [1]:
I performed most of the computations and analyzed the spectra. I wrote a draft for the manuscript, including the figures, and took part in subsequent discussions.

Paper [2]:
I took part at most of the measurements and data analysis and performed the computations. I wrote a draft for the manuscript and was involved in the further discussions.

Paper [3]:
I wrote a draft for the manuscript, as well as performing most of the computations.

Paper [4]:
I contributed at the data measurements, performed computations and was involved in the discussions and writing of the paper.

Paper [5]:
I contributed to the measurements and during discussions and writing of the paper, in particular the parts involving 1,1-dichloroethene, comparison between physisorbed and gaseous states and the relation between hybridization and ionization energy. I also made the figures 1, 5 and 6.

Chapter 1

Introduction

Chlorine is an important substituent in organic chemistry. It has a double nature - on one hand it has strong electron withdrawing abilities and on the other hand, it can donate electrons, both through polarization and also more directly by interaction with a nearby π-system. Hence, it can be both activating and deactivating for a chemical process. A carbon-chlorine bond is relatively weak, making chlorinated compounds a well suited starting point for further functionalization through substitution reactions. Addition of chlorine to a hydrocarbon will increase the polarity of the molecule and can thereby change solubility and interfacial properties.

In the present work, a range of properties for simple chlorinated hydrocarbons have been studied, including core ionization, protonation and electrophilic addition of HCl. The main focus has been the influence of chlorine in each process. As representatives for saturated compounds, the series of chlorinated methanes is included ($CH_{4-n}Cl_n$), while unsaturated chlorinated hydrocarbons are represented by six ethenes and seven propenes. By varying the degree of chlorine substitution in a systematic manner, one can probe corresponding changes in properties and also detect possible interactions between substituents. Computational chemistry has been an integrated tool at every level. Spectroscopic measurements have partly provided complementary information but also served to bridge the gap between the computational and experimental world. Before introducing the topics of research, a brief presentation of the applied spectroscopic technique, namely photoelectron spectroscopy, may be of use.

1.1 X-ray photoelectron spectroscopy

The main idea is simple. An electron is removed by means of radiation, and the kinetic energy of the outgoing electron is measured. Knowing the energy of the radiation, one can calculate the energy by which the electron was bonded to the nucleus. This energy is called the binding energy, or more

commonly, the ionization energy. The removal of an electron, ionization, is often carried out by means of UV-radiation, and then only valence electrons can be removed. If, on the other hand, X-ray radiation is used, the radiation has sufficient energy to remove also inner-shell electrons and the technique is then called X-ray photoelectron spectroscopy, abbreviated XPS.

As an analytical tool, XPS is very powerful. It is element specific for most elements in the periodic table and can provide detailed information about the chemical environment, such as oxidation state or the presence of neighboring atoms (substituents). In the present work, we are investigating organic compounds and will therefore mainly focus on carbon 1s photoelectron spectra. Essential to the interpretation of the spectra is the chemical shift which is a difference in ionization energy. A chemical shift can be caused by a change of substituent that in the next step will influence the electronic environment of that specific atom and thereby how easily electrons can be removed. These influences can be grouped into initial-state and final-state effects (relaxation), depending on whether they influence the charge distribution in the ground state or contribute to lowering the energy of the final state. Hence, XPS provides a localized picture of the electronic environment of a single atom. Fairly small changes in the electronic distribution in a molecule can be probed, such as those caused by the presence of different rotational conformers.[8]

Another important advantage of XPS, is its surface sensitivity. Although X-rays can penetrate further into the bulk, the detection is constrained by the limited ability of photoelectrons to escape from the condensed phase. The higher the energy of the radiation, the more of the surface is accessible. We have typically worked with radiation energies around 330 eV, corresponding to a escape depth of 5-10 Å. For comparison, the longest distance between hydrogen atoms in an ethene molecule is about 3 Å, and hence, we are in the position of observing only a few monolayers.

1.2 Influence of chlorine on a photoelectron spectrum

1.2.1 Chemical shift

Due to chlorine's strong electron withdrawing abilities, there is a large increase in ionization energy for a chlorinated carbon, about 1.5 eV per chlorine. The peaks can therefore easily be distinguished and assigned. These observations stem from the early days of photoelectron spectroscopy.[9] However, since then there has been a large improvement on instrumental resolution, mainly caused by the largely improved radiation sources (synchrotrons) in the 1990's. One has also realized that a photoelectron spectrum is far more rich in information than simply a chemical shift. We have therefore mea-

sured the spectra of the chlorinated methanes (chloromethanes) and ethenes (chloroethenes) at high resolution. In addition, a set of mostly non-published spectra of chlorinated propenes (chloropropenes) are presented. Most of the spectra in this work have a instrumental resolution of 60-70 meV, and this allows us to resolve also vibrational fine-structure in the spectra.

1.2.2 Lifetime of a core hole

When a core electron is removed from a carbon, a short-lived hole state is created. This is an excited state, and it will primarily decay via the Auger process, namely that an outer electron fills the core hole while a second valence electron is ejected from the molecule. The decay rate, can, to a first approximation, be related to the electron density on the ionized atom (one-center Auger decay). According to this model, the electronegativity of chlorine will reduce the electron density on the carbon and thereby increase the lifetime of the core hole.

The excited species has a lifetime of only a few femtoseconds and the lifetime-energy relation states that one cannot know both the energy and the lifetime of a state with unlimited precision: $\Delta E\tau \geq \hbar$. Here, τ is the life-time and $\hbar$ is the reduced Planck constant. ΔE is the range of energies, observed as the peak's full-width at half maximum (fwhm). Hence, the shorter the lifetime, the larger the imprecision in energy, and the larger the broadening of the photoelectron spectrum. For a carbon 1s spectrum, it is typically in the range of 100 meV.[10] Life-time broadening is one of several important parameters when interpreting a spectrum and can be determined only if all other parameters, such as vibrational broadening, instrumental broadening and post-collision interactions, are known. One aim of the present work is to predict accurately the vibrational broadening so that we can determine the lifetime of the C1s hole in the series of chlorinated methanes.

1.2.3 Rotamers

Many molecules undergo torsional vibrations in the ground state. If the potential energy barriers between the torsional minima are sufficiently high, then the rotation is hindered and the molecule possess two or more stable rotational conformers or rotamers. Whereas a methyl group rotates freely at room temperature, chlorine increases the moment of inertia, causing the chloromethyl group to have a hindered rotation. The two molecules with a chloromethyl group, 3-chloropropene and 2,3-dichloropropene, therefore possess two stable rotational conformers.

It is often of interest to decide the relative abundance of rotamers at room temperature. At this temperature NMR cannot be used as the field frequency is usually far too low compared to the frequency of the rotation. IR can be used if the rotation induces significant changes in at least one vi-

bration, as often is the case. Also, gas electron diffraction and microwave spectroscopy can be used, although each of them has their limitations. Regardless of method, an experimental determination of relative populations is a rather demanding task. In principle, theoretical calculations can be used to predict the energy difference between two conformers and in the second step, this can be used as input in the Boltzmann factor to predict relative populations. However, it has proven difficult to predict the energy differences accurately enough to obtain reliable relative populations. A yet different approach is to utilize that the photoelectron spectra of two rotational conformers often will be qualitatively different and that the measured spectrum will be a weighted average of the two individual contributions. Given that we are able to model both of the contributions, the relative populations can be obtained in a least-squares fit of the two model spectra to the experimental spectrum. [8, 11]

1.3 Ionization, protonation and electrophilic addition of HCl

Since the early days of XPS, researchers have sought to relate ionization energies to other chemical properties. Linear correlations between protonation enthalpies and core-ionization energies have been found for nitrogen, oxygen, and phosphorus in a variety of compounds and later also for carbon.[12–24] The rationale for comparing protonation and ionization has been that both processes involve the introduction of a localized positive charge in the molecule. Often the correlations have slopes close to one, interpreted as evidence for a substituent affecting the energies for the processes in a similar way.

The process of protonation is the first step for electrophilic addition of a haloacid, such as HCl, to a molecule in solution.The reaction is regiospecific and depending on the orientation of HCl, the reaction is classified either as Markovnikov or anti-Markovnikov, Markovnikov being the preferred. Again, a localized charge is added to the molecule, and the correlation between activation energies and ionization energies have been investigated along similar lines as the protonation enthalpies. Indeed, linear correlations for addition of haloacids to hydrocarbons have been found, in fact even for gas-phase electrophilic addition where the process is an one-step reaction without the formation of a carbocation.[21, 23, 25, 26]

Holme *et al.* study the addition of HCl to a series of linear alkenes and find certain patterns, as shown in Fig. 9 in Ref. [26]. Firstly, they find a linear correlation between ionization energies and activation energies for Markovnikov addition of terminal alkenes. However, the corresponding anti-Markovnikov energies cluster together well above the line. Furthermore, non-terminal alkenes display a more scattered pattern of points falling above

the line and between the two other groups. From these findings we can deduce that the matter clearly is more complex than a uniform correlation of energies between the two processes.

1.4 Bonding of a chlorinated compound to a semiconducting surface

One of the two most common silicon surfaces is denoted Si(111)-7×7. The term 7×7 reflects the fairly complex reconstruction with a unit cell consisting of 49 atoms. Today, the most widely accepted model of the structure, is the one presented by Takayanagi *et al.*[27] According to their model, the surface has a large variety of binding sites and the same molecule can potentially covalently bond at different sites by different mechanisms.[28]

In the present work, we report on studies of the adsorption, both chemisorption and physisorption, of 1,1-dichloroethene to Si(111)-7×7.[4, 5] When a molecule is covalently bonded to a surface, we say that the molecule is chemisorbed. During chemisorption, internal covalent bonds in the molecule are broken and new bonds between the molecule and the surface are formed. The chemisorbed species has different properties from the free molecule. A spectrum of a chemisorbed species (chemisorption spectrum, for short) is usually different from that of the free molecule, both concerning internal shifts and the shape of individual peaks. [29–31]

The interpretation of spectra of adsorbed species (adsorption spectra) is often complicated by limited resolution. Even if the experiments themselves are of high quality, the polarizable surface induces additional broadening to the spectra that cannot be avoided. It is therefore useful to search for tools that can simplify the interpretation and one common approach is to use computations. Often, a chemisorbed molecule is modeled as attached to e.g. a Si_9H_{12} cluster. However, chemical shifts are often mostly depending on the closest neighbor and we test therefore the validity of a even simpler model, namely to use SiH_3 as a model for the changes in ionization energy caused by a covalent attachment to the surface.

If a molecule is bonded to the surface only by weak van der Waals forces, the molecule is by definition physisorbed. A physisorbed molecule is only slightly perturbed compared to the free molecule, in contrast to the chemisorbed species described above. This could open for another possible approach for interpretation, namely by comparison to gas-phase spectra.[32, 33] By means of theoretical models, high-resolution gas-phase spectra can often be unambiguously interpreted. If this interpretation could be exploited for physisorbed molecules, it would largely simplify the interpretation and increase the level of confidence. For 1,1-dichloroethene we explore the hypothesis that a spectrum of a physisorbed species can be modeled by the corresponding gas-phase spectrum if additional broadening

is included. In reality, the boarder line between chemisorption and physisorption is blurred and many intermediate situations can arise, such as strong hydrogen bonding or weak charge transfer.[34] A close connection between physisorption spectra and gas-phase spectra might also open for the possibility that one is in the position to judge whether a species is truly physisorbed or if other bonding mechanisms are involved.

1.5 Computations and experiments

Sometimes, computations and experiments can provide the same piece of information and can then be used to mutually indicate the quality of the two sets of results. Depending on both the experiment and the computations, one would have to decide which set of data is considered the most reliable. Stochastic errors have a higher occurrence in experimental results, while systematic errors dominate in computed results. Shift in ionization energies, e.g. the energy difference between two peaks in a spectrum, can also be predicted theoretically and one may use the measured shift to decide the quality of the computation.

Often, the matter is even more complex. Not rarely, theoretical models are invoked in the interpretation of data, and it can be hard to decide whether the discrepancies are caused by errors in the model used for interpretation, in the measurements or in the computations. Such a situation arises when one is to interpret high-resolution gas-phase photoelectron spectra. The spectra posses a large amount of fine-structure, and to be able to access the chemical information contained therein, we are depending on computations. All the measured spectra have been interpreted using a large amount of computed information and the experimental information obtained is therefore also partly theory dependent. However, the more complex the fine-structure, the less are the chances that one randomly create a correct model. Correctly predicted geometries is one of the cornerstones to be able to create models that reproduce the spectra. Hence, a good fit is a clear indication of correctly predicted molecular geometries and the spectra can therefore be used indirectly to evaluate computed molecular geometries.

In order to use computations as efficiently as possible, it is useful to be able to perform computations at the desired and well-defined level of accuracy. Chlorine can represent a computational challenge, even the C-Cl bond length in CH_3Cl has proven difficult to predict at a very precise level.[35] Since chlorine is highly polarizable, it demands for polarization functions and diffuse functions, rapidly increasing the computational costs if larger basis sets are used. Also, electron correlation needs to be treated more carefully, leading to more costly methods. Part of our aim is to get insight in how well common methods and basis sets are performing when it comes to geometries and energies of chlorinated compounds. By studying

variations in a systematic manner, one might find corrections that can be applied to related systems.

Chapter 2

High-resolution X-ray photoelectron spectroscopy

X-ray Photoelectron Spectroscopy (XPS), originally called Electron Spectroscopy for Chemical Analysis (ESCA), is a technique dating back to the mid 1960's. The work of Kai Siegbahn and coworkers was awarded the Nobel Prize in Physics in 1981. The technique has several apparent strengths; it is atom-specific for nearly all atoms in the periodic table, has a high surface-sensitivity and can be applied to gas, liquid as well as the solid state. If conventional X-ray sources are used, it can be performed as a home-laboratory experiment. However, to achieve high-resolution spectra where vibrational fine structure is also resolved, monochromatized synchrotron radiation is needed. The photoelectron spectra in the present work were measured at the synchrotron facilities MAX-lab in Sweden and at the Advanced Light Source (ALS) in Berkeley, California. These two facilities are quite similar, and a procedure for uptake of X-ray photoelectron spectra at beamline I411 at MAX-lab is described below.[36, 37] Details about the beamline at ALS, Beamline 10.0.1, can be found in Ref. [38]. XPS measurements of compounds adsorbed to a silicon surface are described in a separate section below.

Except for a chlorine 2p spectrum (Ref. [4]), only carbon 1s photoelectron spectra are included. A carbon 1s spectrum typically consists of several main peaks, one for each chemically unique carbon. As a first approximation, one may assume the relative intensities of the peaks to reflect the stoichiometry of the various carbons. However, it is important to note that several phenomena can alter this ratio significantly, e.g. shake-up/shake-off effects or the more recently discovered phenomena of photon-energy dependent scattering effects.[39]

2.1 Synchrotron radiation

In Fig. 2.1, an overview of the MAX-lab facility is given. Electrons are accelerated to a speed close to the speed of light and inserted in a storage ring by the injector. Beamline I311 is the leftmost beamline, next to I411, and both beamlines are connected to the MAX II storage ring.

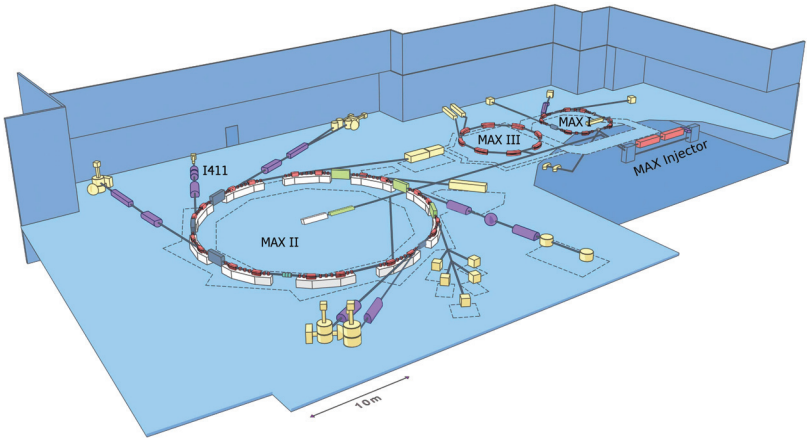

Figure 2.1: An overview of the MAX-lab facility. Reproduced with permission from MAX-lab.

Several devices at an electron storage ring can create synchrotron radiation, so as bending magnets, wigglers and undulators. An undulator consists of a periodic array of magnets. The electromagnetic field enforces the electrons to oscillate and thereby create electromagnetic radiation. By varying the distance between the two arrays, one can adjust the wavelength of the radiation. However, the resulting radiation is still a somewhat broad distribution of wavelengths. One can narrow the distribution through monochromatization and this takes place at the beamline, the straight section departing from the storage ring. The soft X-ray monochromator at beamline I411 is a Zeiss-SX-700 plane grating monochromator and consists of a diffraction grating and an adjustable, narrow slit. At the end of the beamline is an experimental station where the measurements are performed.

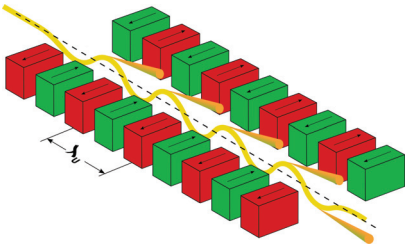

Figure 2.2: An undulator produces radiation by causing a periodic angular acceleration of electrons. Reproduced from Ref. [40].

2.2 Experimental station and acquisition of spectra

The compounds in the present work have a significant vapor pressure at room temperature and are measured in the gas-phase. They are cleaned by freeze-pump-thaw cycles before the vapor is let into a gas cell were it is hit by the incoming radiation. The gas-phase spectra in the present work are measured at 330 eV photon energy. The photoelectrons are analyzed using a Scienta Electron Spectrometer (SES-200). A spectrometer analyzer consists of an electron lens and a detector. The electron lens focuses the electrons towards the entrance slit of the analyzer and also either retards or accelerates the electrons to a known pass energy before they enter the analyzer. The angle between the spectrometer and the analyzer was chosen to be close to 54.7° (the magic angle). At this specific angle, the electron intensity is proportional to the case where electrons are collected over all possible angles.

In the analyzer, the electrons are shielded from the external magnetic field. The electrical field between the two hemispherical electrodes is varied, and electrons of different kinetic energy are detected. The detector is a multichannel detector equipped with a grating to control the incoming direction of electrons. The electrons then pass two micro-channel plates (electron multiplicators) and hit a phosphorous screen thereby creating a flash. These flashes are further detected by a charge-coupled device (CCD) camera and counted. These numbers are the intensities (y) at each energy (x) and constitutes the photoelectron spectrum.

2.3 Calibration

The actual wavelength of the radiation can differ from the set wavelength and it is therefore necessary to calibrate the sample against a calibrant with already known ionization energy that does not overlap with the sample peak. For most carbon 1s spectra, CO_2 is a useful reference compound with a reported ionization energy of 297.664 eV.[41] The calibration was performed by measuring a mixture of calibrant and sample. Also, the CO_2 calibration spectrum provides a useful measure of the instrumental resolution, since this parameter can be left as the only free variable in a least-squares fit to the spectrum. This was of particular use of when determining core-hole lifetimes of chlorinated methanes.[1]

2.4 Experimental procedures for surface measurements

Spectra of 1,1-dichloroethene adsorbed to a Si(111)-7×7 surface were measured at Beamline I311 at MAX-lab. This beamline has an experimental section optimized for surface measurements and is described in Ref. [42]. The Si(111) surface was cleaned by cycles of flashing the surface above 1000°C followed by annealing below 900°C. Silicon 2p spectra were measured to verify that the surface was clean and the 7×7 surface structure was verified. Liquid 1,1-dichloroethene was cleaned by freeze-pump-thaw cycles before exposure.

Chemisorption was carried out by stepwise exposing the surface to a total of 10 L sample at room temperature. Next, the system was cooled to 120 K by means of N_2(l) and spectra of the chemisorbed species were measured. Then, the surface was exposed to another 10 L at 120 K, leading to the formation of a physisorbed layer on top of the chemisorbed molecules. These spectra contain contributions from both the chemisorbed and physisorbed species. Due to low intensity close to the Fermi level, the spectra are plotted on a relative binding energy scale, in lack of a indigenous ionization-energy reference. Carbon 1s spectra were measured at 320 and 330 eV photon energy with estimated resolutions of less than 90 meV. Chlorine 2p spectra were measured at 250 eV photon energy and have a estimated resolution of less than 60 meV.

Chapter 3

Computational

The results of the present work are based on extensive use of quantum chemical calculations. A quantum chemical calculation seeks to solve approximately the Schrödinger equation:

$$\hat{\mathrm{H}}\Psi = \mathrm{E}\Psi \tag{3.1}$$

$\hat{\mathrm{H}}$ is the quantum chemical operator, Ψ is the wave function, and E is the total energy of the system. However, since the equation cannot be solved exactly for many-electron systems, the solution needs to be based on a set of approximations. Firstly, the Born-Oppenheimer approximation states that, due to the large difference in mass between electrons and nuclei, the electrons can be considered to move in a stationary framework of nuclei. As a consequence of this, the total wave function, Ψ, can be separated into one nuclear and one electronic part: $\Psi = \psi_{nuclear} \times \psi_{electronic}$. Different approaches to solving the electronic part of the Schrödinger equation have resulted in several main classes of computational methods, such as Hartree-Fock and post Hartree-Fock *ab initio* methods and density functional theory methods.

The present chapter starts with a very brief presentation of the main computational methods used throughout the work, emphasizing the differences between them. It will also give an overview of the wave function descriptions, namely the basis sets. Finally, it seeks to give the reader the necessary details about how various chemical properties, such as ionization energies, geometries, protonation enthalpies and activation energies, are computed. Unless explicitly stated, the computations are performed using the Gaussian package of programs, G03 or G09.[43]

3.1 Computational methods

3.1.1 Hartree-Fock

Hartree-Fock (HF) is the foundation for all the other methods used in this work. It is based on the Hartree-Fock assumption, namely that the true wave function for a system can be approximated by an antisymmetrized product of one-electron wave functions, a Slater determinant. According to the variational principle, the correct solution to the Schrödinger equation is approached by varying the wave functions so that the total energy (E) is minimized.

The Hartree-Fock operator, $\hat{\mathrm{f}}$, is a one-electron operator and can be expressed as

$$\hat{\mathrm{f}} = \mathrm{T_e} + \mathrm{V_{Ne}} + \mathrm{V_{HF,ee}} \tag{3.2}$$

$\mathrm{T_e}$ is the kinetic energy of the electron and $\mathrm{V_{Ne}}$ is the potential energy due to the electron-nucleus attraction. $\mathrm{V_{HF,ee}}$ is the Hartree-Fock potential which is the repulsive potential experienced by one electron due to the average positions of every other electrons in the molecule. $\mathrm{V_{HF,ee}}$ can further be separated into two components. The first component is the sum of pairwise coulomb repulsions between the electron and every other electron. The second component is the exchange potential (E_X^{HF}).

In HF it is assumed that the total wave function can be separated into one-electron wave functions. If this were correct, it would imply that each electron behaves independently from the others, which it does not. As a consequence, the HF energy ($\mathrm{E_{HF}}$) is always higher than the true energy ($\mathrm{E_0}$). Löwdin called this difference the correlation energy: $\mathrm{E_{corr}} = \mathrm{E_0} - \mathrm{E_{HF}}$.[44] The electron correlation energy increases in magnitude with the number of electrons and with increasing electron density.

The correlation energy can be discussed in terms of dynamical and static electron correlation.[45] Dynamical correlation is the far most important and is related to the fact that there is instantaneous repulsion between the electrons. HF does not take into account that due to this repulsion the electrons instantaneously adjust their positions so as to minimize the total energy. As a consequence, the electron-electron repulsion included in HF is too large and therefore also the total energy, E_{HF}. The second contribution to the correlation energy, static correlation, becomes important when different electron configurations are close in energy so that the system can be in different states. Then a single Slater determinant cannot be qualitatively correct and the HF approach leads to a wrong description of chemical properties such as for example geometries.

Post-Hartree-Fock methods and density functional theory methods seek to reduce the HF discrepancies through different approaches, and we focus in the following on how the the dynamical correlation is treated.

3.1.2 Post Hartree-Fock methods

A Mller-Plesset (MP) calculation consists of a HF calculation followed by a calculation of the correlation energy correction by means of perturbation theory.[46] The perturbed wave function and perturbed energy are expressed as power series in the perturbation, which in MP is the difference between the correct electron-electron repulsion operator and a sum of Hartree-Fock potentials (one for each electron). The MP method is further named after the highest power that is retained in these power series, i.e., the truncation level. Two different MP methods were used in this work, namely MP2 and MP4(SDQ). MP2 includes only second-order corrections to the energy.[47] MP4(SDQ) is truncated after the fourth-order terms, but it is not a full MP4 as it only includes single, double and quadruple excitations of electrons into virtual orbitals.

Another important group of methods are the coupled clusters methods. They use an exponential cluster operator to account for dynamic electron correlation in terms of excitations into virtual orbitals to create a new wave function. We have used CCSD(T), coupled clusters with singles and doubles and perturbative treated triples excitations.[48] Also included in CCSD(T) are the products of single- and double excitations, so that higher order excitations to some extent is included.

Coupled clusters and MP methods increase rapidly in computational costs as higher orders of electron correlation are included and the most accurate computations are only possible for rather small chemical systems.

3.1.3 Density functional theory

Density functional theory (DFT) commonly replaces the HF electron-electron repulsion term, $V_{HF,ee}$, in the HF operator (Eq. 3.2) with new terms to include both electron correlation and exchange energy. We have applied the Becke three parameter hybrid functional B3LYP.[49] It is called a hybrid functional because it includes a mixture of HF exchange and DFT exchange-correlation. Three (3) constants (a_0, a_x and a_C) are obtained by optimization of results towards a set of experimental data.

$$a_0 \cdot E_X^{Slater} + (1-a_0) \cdot E_X^{HF} + a_X \cdot \Delta E_X^{Becke} + a_C \cdot E_C^{LYP} + (1-a_C) \cdot E_C^{VWN} \quad (3.3)$$

The subscripts X and C denotes exchange and correlation, respectively. B3LYP uses the non-local correlation provided by the LYP expression developed by Lee, Yang, and Parr.[50] Local correlation is described partly by local terms included in LYP and partly by the VWN functional III. [51]

3.2 Basis sets

When performing a quantum mechanical calculation, the wave functions are expressed in terms of molecular orbitals, which in turn are found as linear combinations of predefined functions. These functions constitutes a basis set and the more basis functions, the larger the flexibility. However, a larger number of basis functions also increases the computational cost and one therefore often wants to increase the flexibility in regions where the benefits are the largest. Commonly, a basis set is improved by adding extra polarization functions or diffuse functions. Polarization functions allows for a more asymmetrical electron distribution whereas diffuse functions extend over a larger radial distance from the nucleus. An overview of the most frequently used basis sets in the present work, is given in Tab. 3.1. Here, the *aug* prefix indicates that the basis set includes diffuse functions. Since the cc-pVTZ and cc-pVQZ sets do not include tight polarization functions, an extra tight d-function is added for chlorine (+d).

When computing theoretical ionization energy shifts for chemisorbed 1,1-dichloroethene,[4] the 6-311G(d) basis was used for silicon.[52] The remaining atoms were represented by the tzp basis described above.

It should be added that a large basis set usually is more important for post-Hartree-Fock methods than for density functional methods.[53] Therefore, it was considered sufficient to use the tzp basis for most B3LYP calculations, although the basis did not perform well for CCSD(T) calculations on chlorinated compounds.

Table 3.1: Overview of the most important basis sets in this work

Designation	Atom	Details	Primitive basis	Contracted basis	Ref.
tzp	C	Cf [1]	11s,6p,1d	5s,3p,1d	[52, 54]
	H	Cf [2]	5s,1p	3s,1p	[52, 54]
	Cl	Cf [3]	13s,10p,2d	6s,5p,2d	[55–57]
(aug-)cc-pV(T+d)Z	C	cc-pVTZ	19s,6p,3d,2f	5s,4p,3d,2f	[58]
	H	cc-pVTZ	6s,3p,2d	4s,3p,2d	[58]
	Cl	aug-cc-pV(T+d)Z	42s,17p,4d,2f	6s,5p,4d,2f	[59]
(aug-)cc-pCV(T+d)Z	C	cc-pCVTZ	20s,7p,3d,1f	6s,5p,3d,1f	[58]
= aug-TZ	H	cc-pVTZ	6s,3p,2d	4s,3p,2d	[58]
	Cl	aug-cc-pV(T+d)Z	42s,17p,4d,2f	6s,5p,4d,2f	[59]
cc-pC*V(Q+d)Z	C	cc-pC*VQZ[4]	13s,7p,4d,3f,2g	6s,5p,4d,3f,2g	[58]
=QZ	H	cc-pVQZ	7s,3p,2d,1f	4s,3p,2d,1f	[58]
	Cl	cc-pV(Q+d)Z	16s,11p,4d,2f,1g	6s,5p,4d,2f,1g	[59]
(aug)-cc-pCV(Q+d)Z	C	cc-pCVQZ	24s,9p,5d,3f,1g	8s,7p,5d,3f,1g	[58]
= aug-QZ	H	cc-pVQZ	7s,3p,2d,1f	4s,3p,2d,1f	[58]
	Cl	aug-cc-pV(Q+d)Z	33s,20p,5d,3f,2g	7s,6p,5d,3f,2g	[59]

[1] C: Dunning triple zeta basis plus single set of polarization functions (d).
[2] H: Dunning triple zeta basis plus single set of polarization functions (p).
[3] McLean and Chandler triple zeta plus doubly split polarization functions.
[4] Additional contracted [3s,3p,2d,1f] included for the ionized state.

3.3 Ionization energies and geometries

As the core of each ionized atom is represented by an effective core potential described below, only relative ionization energies can be computed. In most cases, geometries were optimized at the CCSD(T)/tzp level and the energies found in single-point calculations in this geometry. Corrections for zero-point vibrations were computed at the B3LYP/tzp level of theory.

3.3.1 Hole-state calculations

The core of the ionized carbon was represented using the effective core potential (ECP) of Stevens *et al.* scaled to account for only one electron in the 1s shell.[60, 61] The validity of the ECP model for computing energies and geometries was explored by a series of hole-state calculations at the HF-level.[1, 2] These were conducted using the Dalton package of programs.[62]

3.3.2 Additional corrections

For the chlorinated methanes, the effect of basis-set superposition errors (BSSE) on geometries were accounted for by counterpoise corrections.[63]

The most significant contributions to electron correlation comes from interactions between valence electrons and the default setting in Gaussian is to include only this interaction. When computing geometries of the chlorinated methanes, also core-core and core-valence correlation corrections were computed at the MP2 level. In addition, they were computed at the CCSD(T) level for chloromethane and dichloromethane.

3.4 Extended Koopman's theorem

If one substituent is interchanged with another, the resulting shift in ionization energy (ΔIE) is partly caused by a new charge distribution in the ground state (ΔV) and partly by a different pattern for charge delocalization in the final state (ΔR). These contributions are commonly referred to as initial- and final-state effects and the relation can be written
$\Delta IE = \Delta V - \Delta R$.

Koopman's theorem states that the initial state potential is given by the orbital energy, ϵ_c. To also include electron correlation, an extended version of Koopman's theorem (EKT) was developed [64]:

$$\Delta V^{EKT} = -\Delta\epsilon_c + \Delta(U^{corr} - U^{HF}) \tag{3.4}$$

U is the electrostatic potential at the site of ionization. U^{HF} is computed using Hartree-Fock (HF) while U^{corr} is the potential computed using an electron correlation method, in the present case MP4(SDQ). ΔR was calculated

as the difference between ΔV^{EKT} and the experimental shift, ΔIE. Usually, ΔV^{EKT} is referred to as ΔEKT.

3.5 Protonation enthalpies

Protonation enthalpy, ΔH_{prot}, is the enthalpy of the reaction of adding a proton (H^+) to a species and is the negative of the proton affinity. The protonation enthalpies were computed as the difference in enthalpy between the protonated state and the two ground-state species, a neutral molecule and a proton. The enthalpies were calculated by means of Gaussian-4 theory (G4)[65]. The temperature was set to 298 K and the enthalpy of the proton was predicted as (5/2)RT.

3.6 Activation energies for electrophilic addition

Activation energies (E_a) for the addition of HCl to chlorinated ethenes and propenes, as well as to ethene and propene and 2-methylpropene, were computed as the difference in energy between the ground-state species and the transition-state complexes. Gas-phase geometries were optimized using B3LYP/tzp. Next, single-point energies for the species were computed using CCSD(T)/aug-TZ. To obtain corrections for basis set incompleteness, single-point energies were computed at the MP4(SDQ) level using aug-TZ and aug-QZ. In addition to these corrections, the final estimates of the gas-phase activation energies also included thermal corrections at 298 K.

To mimic the effect of a solvent phase, the scrf keyword (self consistent reaction field) in G09 was used. The geometries were re-optimized in two different polar surroundings according to the Polarizable Continuum Model using the integral equation formalism variant (IEFPCM).[66] Solvent parameters corresponding to 1,1,1-trichloroethane were chosen, and the cavities were defined using the United Atom Topological Model (UA0). The solvent-state energies were used without any further corrections.

Chapter 4

Analyzing a photoelectron spectrum by means of theoretical lineshapes

The previous two chapters describe how photoelectron spectra are recorded and give a brief introduction to the computational methods that are used in this thesis. The present chapter seeks to bring these two together and describe how theoretical computations are used in the interpretation of the experimental data. Our aim is to extract an ionization energy for each chemically inequivalent site in a molecule from a spectrum. To be able to do so, we predict a theoretical vibrational lineshape for each site based on the Franck-Condon principle that will be described below.

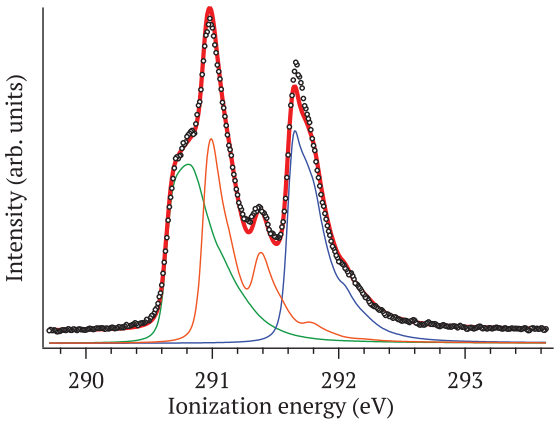

Figure 4.1: Carbon 1s spectrum of *trans*-1-chloropropene. The overall fit (red line) to the experimental data (circles) is the sum of three theoretical vibrational lineshapes, C1 (blue), C2 (green) and C3 (orange), and a constant background. Ref. [2].

Fig. 4.1 displays the experimental carbon 1s photoelectron spectrum of *trans*-1-chloropropene, HClC=CH-CH_3. The peak at highest energy can unambiguously be assigned to C1 due to the higher electronegativity of chlorine. The low-energy peak contains contributions from both C2 and C3. It has a shoulder at lower binding energy and a distinct feature at 291.4 eV. Included in the figure are also the three theoretical lineshapes used to fit the spectrum (thin lines) and the resulting model spectrum (thick, red line). The model spectrum does not constitute a perfect description of the experimental spectrum, and in particular the peak assigned to the chlorine-substituted carbon is less well represented. However, the lineshapes are quite different and can by no means be interchanged, so the peaks can be unambiguously assigned. Furthermore, the description at the low energy-side of each peak is the most important, and since this is well described, we know from experience that the uncertainty in ionization energy will be less than 50 meV.

4.1 The Franck-Condon principle

Why do the theoretical lineshapes in Fig. 4.1 look different, and how can they be predicted? A spectrum of a single atom may very well consist of only a single line but when a molecule is ionized, it will often also start vibrating. The additional energy involved in the vibrational excitation will decrease the kinetic energy of the outgoing photoelectron and the corresponding signal will appear as a satellite peak at higher energy in the spectrum. To interpret the vibrational fine structure of the spectrum, we can predict the positions and intensities of these additional satellites, or, in other words, construct a theoretical vibrational lineshape.

Each vibrational state of a molecule is described by a vibrational wave function, $|\nu\rangle$. We denote the vibrational wave functions of the ground state $|\nu_i\rangle$ and those of the final state $|\nu_f\rangle$. Fig. 4.2 is an illustration of the Franck-Condon principle for an one-dimensional case. As often is the case, the potential energy surfaces of the two states are approximated by harmonic potentials. The lowest vibrational states, $|\nu_{i0}\rangle$ and $|\nu_{f0}\rangle$, are the zero-point vibrational states and a transition between these is an adiabatic transition. The adiabatic ionization energy is the energy required to perform this transition, and although not explicitly stated above, this is the energy we would like to extract from our spectra. For XPS measurements performed at low resolution, vertical ionization energies are usually reported. The vertical ionization energy is the average ionization energy when all vibrational excitations are included.

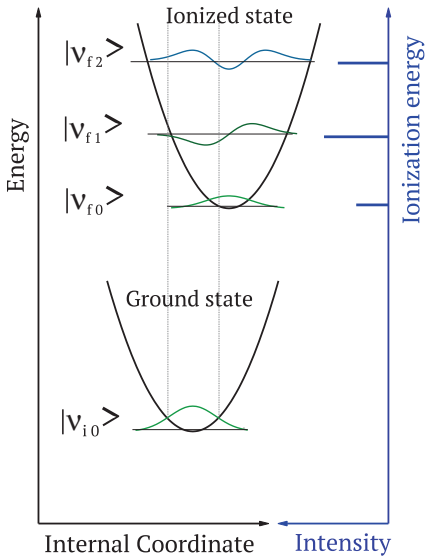

Figure 4.2: The Franck-Condon principle illustrated for an one-dimensional case.

The Franck-Condon principle states that the probability for a given transition, is given as the squared overlap integral between the two vibrational wave functions, illustrated by the two grey lines in Fig. 4.2. The energy positions of each satellite relative to the adiabatic transition becomes $(\epsilon_{\nu_f} - \epsilon_{\nu_i}) - (\epsilon_{0_f} - \epsilon_{0_i})$. If we perform a full Franck-Condon analysis, we get a theoretical vibrational lineshape, analogous to the one illustrated in blue to the right in the figure.

4.2 Broadening of a photoelectron spectrum

However, neither the experimental spectrum nor the lineshapes in Fig. 4.1 appears as a set of sharp peaks similar to those to the right in Fig. 4.2. Firstly, the incoming radiation is not perfectly monochromatized, and contributions from the analyzer and detector induces additional uncertainty to the measured kinetic energy. The sum of these contributions, commonly referred to as instrumental broadening, is usually well represented by a Gaussian-shaped broadening function. Secondly, even if we could perform a measurement with infinite accuracy, we could not avoid life-time broadening. Thirdly, a carbon atom will relax from the excited core-hole state by emitting an Auger electron. If the photoelectron is overtaken by the Auger electron, it experiences a effective potential of +2 and is retarded. In the spectrum, this is observed as an asymmetry of the peak and the phenomena is often referred to as post-collision interactions.

4.3 Overview of the Franck-Condon analysis

Geometries of the neutral ground and ionized states are optimized and for each stationary state, normal modes and harmonic normal mode frequencies are predicted at the B3LYP/tzp level. In a second step, geometries were re-optimized at a higher level using CCSD(T)/tzp or better. Finally, B3LYP/tzp normal modes and normal mode frequencies were combined with changes in geometries computed at the higher level. All C-H contractions for the ionized carbons (C*) are reduced by 0.3 pm for sp^3-hybridized carbons and 0.2 pm for sp^2-hybridized carbons to account for neglect of core-core and core-valence correlation and basis set deficiencies. [61] All frequencies are scaled by a factor of 0.99 to correct for systematic errors and the frequency of the symmetric C*-H stretching mode is scaled by an additional factor of 0.97 for sp^2- and 0.96 for sp^3-hybridized carbons.

Normal modes in the initial and final states are paired off and Franck-Condon integrals are computed in the harmonic approximation for most vibrational modes. One exception is the symmetric C*-H stretching mode which is described by a Morse potential. For the chlorinated ethenes, normal modes and the differences in equilibrium geometries were expressed in Cartesian coordinates. For the chlorinated methanes and propenes, normal coordinates were expressed in internal coordinates by means of the ASYM program [67] and internal coordinates also used in the subsequent steps.

Fitting of theoretical lineshapes to the experimental spectra are performed by a least-squares procedure as implemented in the SPANCF package written for Igor Pro (Igor Pro 6).[68, 69] Life-time broadening and post-collision interactions are described by the combined function of van der Straten *et al.*[70] The lifetime width was constrained to 100 meV for non-chlorinated carbons [71, 72] and reduced by 10 meV per chlorine directly attached to the ionized carbon.[1] The Gaussian width was either a free parameter equal for all atoms or it was constrained to the value obtained from analyzing the CO_2 peak in the calibration spectrum.[1]

4.4 Possible shortcomings

Imperfections in a model spectrum, such as those shown in Fig. 4.1, may originate from one or more of the approximations invoked when applying the Franck-Condon principle to a system with multiple vibrations. For the chloromethane series, we aim to estimate the lifetime broadening and therefore need to predict the vibrational lineshape as accurately as possible. With this aim, it is useful to evaluate every possible source of inaccuracy in the predicted lineshape and the present section seeks to give a short overview of possible shortcomings in our standard procedure.

Firstly, the intensities of a vibration is to a large extent depending on a

correct prediction of the *change* in geometry upon ionization and as a rule of thumb, changes in bond distances should be correct within 0.1 pm for a precise description. Here, the choice of electron structure method and basis set is important and also the approximations often applied therein. The effective core potential used to describe the core of the ionized atom may be a possible source of error, as well as lack of correlation for inner electrons and neglect of basis-set superposition errors. Secondly, there is a choice of electronic structure method for computing normal modes and normal-mode frequencies and also a choice if these should be computed in the harmonic model. After computing the potential energy surface (PES), it is approximated by a function, usually a harmonic potential. As for symmetric C*-H stretching, a Morse potential may be more appropriate. Thirdly, there is a choice whether normal modes and changes in equilibrium geometries upon ionization are to be expressed in internal or Cartesian coordinates. Curved motions are difficult to describe in Cartesian coordinates as they simply will describe a linear motion between two points and the representation is further deteriorated for large displacements. Bond angles and dihedral angles are curvilinear coordinates and intrinsically describe a curved vibrational path for an atom. Internal coordinates will improve on this by expressing the motion as a change in angle. When mapping final-state normal coordinates onto initial-state coordinates, we obtain a Duschinsky matrix. In the further treatment, after resorting modes to make the diagonal of the Duschinsky matrix as dominant as possible, off-diagonal elements are usually neglected, implying that we are neglecting rotation of vibrational modes between the two states. Also, thermal effects are usually neglected and we consider then only transitions from $|\nu_{i0}\rangle$. However, as an example, 1,1-dichloropropene turned out to have significant thermal excitation in the ground state and a different treatment is then necessary. [2]

Chapter 5

Major results

In the present chapter, some of the most important results from Refs. [1–5] are reported and discussed. Firstly, the role of chlorine as a substituent in each of the three processes core ionization, protonation and electrophilic addition is analyzed. Next, similarities and differences in how chlorine behaves in the three processes are highlighted. The accuracy of computed energies and geometries for chlorinated compounds are evaluated based on measured energies and their abilities to reproduce experimental spectra. Lifetimes for the core holes of chlorinated methanes are measured and the relative populations of the stable conformers of 3-chloropropene and 2,3-dichloropropene are determined from their C1s spectra. Finally, we report results for adsorption of 1,1-dichloroethene on a Si(111)-7×7 surface as studied by XPS.

5.1 Carbon 1s ionization energies

Carbon 1s (C1s) photoelectron spectra are recorded for four chlorinated methanes, namely CH_3Cl, CH_2Cl_2, $CHCl_3$, and CCl_4.[1] Also, C1s spectra for six chlorinated ethenes ($C_2H_{4-n}Cl_n$) and seven chlorinated propenes are recorded.[2] The instrumental resolution of the spectra are in the range 60-80 meV. The spectra are analyzed by means of theoretical vibrational lineshapes to obtain accurate C1s ionization energies. The absolute uncertainty in the energies is about 0.03 eV while the relative uncertainty may amount to 0.02 eV. To account for the possibility that it is lower, ionization energies are quoted by three decimals.

5.1.1 Chlorinated methanes

C1s ionization energies of the four chlorinated methanes as reported in Ref. [1] are included in Tab. 5.1. Also included are ionization energies relative to methane. Rightmost in the table, ionization energies computed relative to the compound with one less chlorine are listed.

Table 5.1: *Absolute and relative carbon 1s ionization energies for chlorinated methanes (eV).*

Molecule	IE	ΔIE[a]	Increase[b]
CH_3Cl	292.321	1.632	1.632
CH_2Cl_2	293.774	3.085	1.453
$CHCl_3$	295.092	4.403	1.318
CCl_4	296.307	5.618	1.215

[a]Computed relative to methane, 290.689 eV, c.f. Ref. [41].
[b]Computed relative to the chlorinated methane with one less chlorine.

The average increase in ionization energy per chlorine is 1.45 eV, but as also is illustrated in Fig. 5.1, the increase in ionization energy is leveling off as the number of chlorines is increasing. The increase in ionization energy of chloromethane compared to methane, is 1.632 eV. For dichloromethane, the increase is 0.179 eV lower than twice the effect of one chlorine. We may think of this as the action of one chlorine being modified by the presence of a second chlorine, or more correctly, as a mutual interaction between the two substituents. We may think of 1.632 eV as the substituent parameter for chlorine and 0.179 eV as an interaction parameter. If we apply these two parameters for trichloromethane, we obtain: $(3 \times 1.632 + 3 \times -0.179)$ eV $= 4.359$ eV. This is only 0.044 eV lower than the measured relative energy. Including interactions between every pair of chlorines, we obtain for tetrachloroethene 5.454 eV which is 0.164 eV lower than the measured shift. Hence, our model is able to predict triple but not quadruple substitution. One possible explanation may be found when comparing Mulliken charges for carbon computed using (aug)-cc-pV(T+d)Z. They are 0.21, 0.36, 0.42 and 0.42 for $n_{Cl} = 1, 2, 3, 4$, respectively, effectively reducing the charge per chlorine throughout the series. [1] As the amount of charge per chlorine is decreasing, the influence of a chlorine on the ionization energy and the mutual interactions between chlorines must change correspondingly.

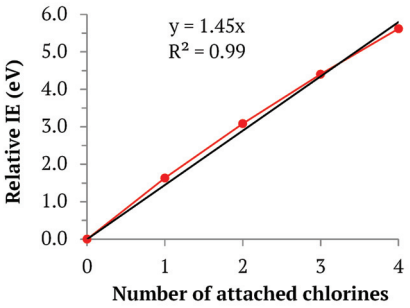

Figure 5.1: C1s ionization energies for methane and chlorinated methanes. The black line represents a first-order regression to the data.

The ionization energies above could have been fitted using a linear regression including higher-order terms to account for interactions between

parameters as described in Ref. [73]. However, then the interactions parameters are averaged so as to suit the complete set of data. This will deteriorate the description for less substituted compounds in favor of describing the more anomalous multiple-substituted compounds. We choose therefore in the present work to analyze also the chlorinated ethene and propene ionization energies in terms of additivity and departure from additivity for single and double substitution. Finally, the model is tested for multiple substitution.

5.1.2 Chlorinated ethenes and propenes

The measured adiabatic C1s ionization energies for the six chlorinated ethenes and seven chlorinated propenes are included in Tab. 5.2.[2] In addition, we rely on previously published ionization energies for ethene [41] and propene.[21]

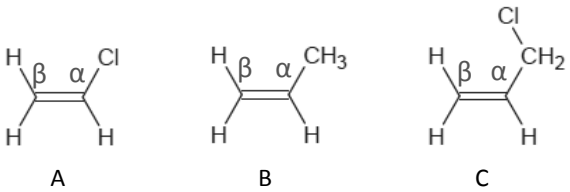

Figure 5.2: Ethene substituted with chlorine (A), methyl (B), and chloromethyl (C).

For the sp^2 carbons, we may analyze the ionization energies along the same line as described for the chloromethanes above. Although the complexity is slightly larger, all the compounds can be thought of as ethene where one or more of the hydrogens are replaced by either chlorine, methyl or chloromethyl. Next, these substituents are categorized as being either in α or β position to the site of ionization, e.g. either attached to the ionized carbon or to the neighboring sp^2 hybridized carbon. For simplicity, a substituent in the α position is denoted as an α substituent, and similarly for β.

A substituent may act both by changing the ground-state electrostatic potential and by contributing to relaxation upon ionization. Ground state potentials were computed by means of the Extended Koopman's theorem described in Sec. 3.4. The resulting ΔEKT may be thought of as the change in potential when substituting ethene with either of the substituents. The relative relaxation, ΔR, is computed as: $\Delta R = \Delta EKT - \Delta IE$.

Table 5.2: *Adiabatic carbon 1s ionization energies (eV) for chlorinated ethenes and propenes. From Ref. [2].*

Molecule		IE	ΔIE [1]	Ref.
Propene	C1	290.136	-0.559	[21]
	C2	290.612	-0.083	[21]
	C3	290.671	-0.024	[21]
Chloroethene	C1	292.203	1.508	[2]
	C2	290.744	0.049	[2]
Cis-1,2-dichloroethene		292.148	1.453	[2]
Trans-1,2-dichloroethene		292.162[2]	1.467[2]	[2]
1,1-Dichloroethene	C1	293.516	2.821	[5]
	C2	290.761	0.066	[5]
Trichloroethene	C1	293.428	2.733	[2]
	C2	292.138	1.443	[2]
Tetrachloroethene		293.435[2]	2.740[2]	[2]
Cis-1-chloropropene	C1	291.626	0.930	[2]
	C2	290.666	-0.029	[2]
	C3	290.782	0.087	[2]
Trans-1-chloropropene	C1	291.619	0.924	[2]
	C2	290.663	-0.032	[2]
	C3	290.949	0.254	[2]
2-Chloropropene	C1	290.304	-0.391	[2]
	C2	292.100	1.405	[2]
	C3	291.081	0.386	[2]
3-Chloropropene, *gauche*	C1	290.496	-0.199	[2]
	C2	290.949	0.254	[2]
	C3	292.201	1.506	[2]
3-Chloropropene, *syn*	C1	290.355	-0.340	[2]
	C2	290.885	0.190	[2]
	C3	292.204	1.509	[2]
1,1-Dichloropropene	C1	292.963	2.268	[2]
	C2	290.747	0.052	[2]
	C3	290.948	0.253	[2]
Cis-1,3-dichloropropene	C1	291.998	1.303	[2]
	C2	290.986	0.291	[2]
	C3	292.275	1.580	[2]
2,3-Dichloropropene, *anti*	C1	290.472	-0.223	[2]
	C2	292.323	1.628	[2]
	C3	292.550	1.855	[2]
2,3-Dichloropropene, *gauche*	C1	290.596	-0.099	[2]
	C2	292.397	1.702	[2]
	C3	292.512	1.817	[2]

[1] Ionization energies computed relative to ethene, 290.695 eV, cf. Ref. [41].
[2] Here, the uncertainty is about 0.04 eV for absolute energies and 0.03 eV for relative energies.

Effect of single substitution: Substituent parameters

Fig. 5.2 illustrates the three single-substituted compounds, namely chloroethene (A), propene (B) and 3-chloropropene (C). 3-Chloropropene possess two stable conformers at room temperature. The chemical shift between these is significant and therefore they both need to be included. The substitution parameters, computed as shifts relative to ethene, are given in Tab. 5.3.

Table 5.3: *Substitution parameters (eV) for X–HC_α=$C_\beta H_2$. From Ref. [2].*

Substituent	ΔIE		ΔEKT[a]		ΔR[b]	
Carbon site→	α	β	α	β	α	β
Cl	1.51	0.05	1.92	0.48	0.41	0.43
CH_3	-0.08	-0.56	0.15	-0.28	0.23	0.28
CH_2Cl, *gauche*	0.25	-0.20	0.66	0.35	0.41	0.55
CH_2Cl, *syn*	0.19	-0.34	0.61	0.10	0.42	0.44

[a]Calculated using MP4(SDQ)/(aug-)TZ.
[b]ΔR = ΔEKT - ΔIE

We observe, as already early discovered [9], that the direct influence of a chlorine is to increase the ionization energy of the carbon to which it is attached by approximately 1.5 eV. This is primarily an initital-state effect amounting to 1.92 eV modified by a relaxation of 0.41 eV. Seemingly, a β chlorine does to a little extent influence the ionization energy, introducing only a small positive shift of 0.05 eV. In reality, a rather large influence (0.48 eV) on the initial-state potential is nearly canceled by relaxation (0.43 eV). Noteworthy, the relaxation caused by chlorine is of similar magnitude both to the α and β position.

The net effect of a methyl group is to decrease the ionization energy. In contradiction to chlorine, the effect is larger when methyl is in β position (-0.56 eV) compared to α (-0.08 eV). The large β shift is caused by a charge donation both in the ground state and upon ionization, the two being of similar magnitude. An α methyl is slightly electronegative in the ground state but is even a more efficient electron donor upon ionization.

Averaging *gauche* and *syn*, the influence of chloromethyl is intermediate to that of chlorine and methyl, increasing the ionization energy of the α carbon by about 0.2 eV and decreasing it by approximately -0.3 eV for the β carbon. Both in α and β position, the electron withdrawing abilities are about 1/3 of that of chlorine while the donating abilities are of comparable magnitude to that of chlorine but smaller than that of a methyl.

Chloromethyl allows us to evaluate also the more distant effect of a chlorine. Comparing *syn* and *gauche*, we observe that there is indeed an influence on the ionization energies induced by the position of chlorine, primarily in the initial state. Furthermore, both the initial- and the final state is of the β site are more influenced than those of the α site. This is consistent with

an expectation of a through-space interaction between the terminal chlorine and a carbon to be larger for C_β than C_α.

Effect of double substitution: Interaction parameters

We focus here on the interactions between chlorine and the other substituents. We assume that the substituent parameters in Tab. 5.3 are additive and that departure from additivity carry information about the interaction between substituents in a similar manner as described above for chloromethane. The upper part of Tab. 5.4 includes the interaction parameters for substituents being on the same carbon as chlorine, e.g. $\overset{Cl}{\underset{X}{}}>C_\alpha{=}C_\beta H_2$. In the lower part, the substituents are on neighboring carbons: Cl–C_αH=C_βH–X. ΔIE, ΔR, and ΔEKT are defined as being α or β relative to the position of the first chlorine.

Table 5.4: *Cl–X Substituent interaction parameters (eV). From Ref. [2].*

Cl–X Interaction	ΔIE		ΔEKT[a]		ΔR[b]	
Carbon site→	α	β	α	β	α	β
$\overset{Cl}{\underset{X}{}}>C_\alpha{=}C_\beta H_2$:						
Cl–Cl	-0.20	-0.03	-0.26	-0.15	-0.07	-0.12
Cl–CH_3	-0.02	0.12	-0.02	0.02	0.00	-0.10
Cl–CH_2Cl, *gauche*	-0.06	0.05	-0.15	-0.08	-0.09	-0.13
Cl–CH_2Cl, *anti*	-0.07	0.07	-0.11	-0.08	-0.04	-0.15
Cl–C_αH=C_βH–X :						
trans-Cl–Cl	-0.09		-0.12		-0.03	
cis-Cl–Cl	-0.10		-0.17		-0.07	
trans-Cl–CH_3	-0.03	0.00	-0.09	-0.09	-0.06	-0.09
cis-Cl–CH_3	-0.02	0.01	-0.02	-0.01	-0.01	-0.01
cis-Cl–CH_2Cl	-0.01	-0.01	-0.10	-0.08	-0.09	-0.07

[a] ΔEKT is calculated using MP4(SDQ)/(aug-)TZ.
[b] ΔR = ΔEKT - ΔIE

The uncertainties are estimated to be in the range 0.05 eV or less, and we discuss in the following only values of larger magnitude. Firstly, it is important to notice that most of the interaction terms are small compared to the first-order effects presented in Tab. 5.3. Secondly, all values for ΔEKT are negative, meaning that one or both of the substituents are able to withdraw less electrons compared to the single-substituent situation. Also, the donation of electrons upon ionization gets less effective, as seen from the generally negative ΔR values.

Looking at two substituents located on the same carbon, the largest interactions are found for two chlorines at the same carbon, amounting to a

reduction in ionization energy of -0.20 eV at the α position. As can be seen from ΔEKT, this is mainly an initial-state effect. Moreover, it is close to the interaction parameter of 0.179 eV obtained for CH_2Cl_2 above. Hence, it is reasonable that the interaction is to a small extent influenced by the π bond but rather is caused by a competition for electrons through the C-Cl bonds. Seemingly, the same two chlorines acting on the β site have an insignificant influence. However, in this case, there is a canceling between initial- and final-state effects, amounting to -0.15 eV and -0.12 eV, respectively. The interaction terms between chlorine and each of the substituents methyl and chloromethyl are positive when they act on the β site and the reason is a less effective relaxation. A further analysis indicates that this stems from a reduced electron donation through conjugation, probably both from chlorine and methyl.

If the two substituents are located at different carbons, the interactions are generally smaller than when they are on the same carbon. Again, the largest interactions are found between two chlorines, reducing the ionization energy by about -0.10 eV relative to a pure additive situation, with a marginally small difference between *cis* and *trans*. For the remaining substituents, initial- and final-state effects cancel, and the influences on the ionization energies are insignificant.

Multiple substitution: Exploring the validity of the parameters

1,1-Dichloropropene, trichloroethene and tetrachloroethene all have a higher degree of substitution and we use these as a testing ground for how well our substituent- and interaction parameters are able to reproduce shifts relative to ethene. We assume that the interaction parameters may be added so as to describe every pair-wise interaction between substituents in the molecule. Hence, for 1,1-dichloropropene, the ionization energy at C1 may be predicted as [2×1.51 + (-0.56)] + [(-0.20) + 0.01 + 0.00] = 2.27 eV, similar to the measured shift. Performing a similar analysis for the other three carbons in the triply substituted compounds, the model predicts results that are 0.05 eV lower than the measured energies. Going to tetrachloroethene, the similar deviation is -0.23 eV. Although the compound is four-fold substituted with the substituent causing the largest deviations, these results indicate a limitation of our simple additivity model when extending to more than three-fold substitution.

5.2 Protonation

Protonation enthalpies are computed by means of Gaussian-4 (G4) theory for chlorinated ethenes and propenes, as well as ethene, propene, and 2-methylpropene. Optimized structures for most protonated species are

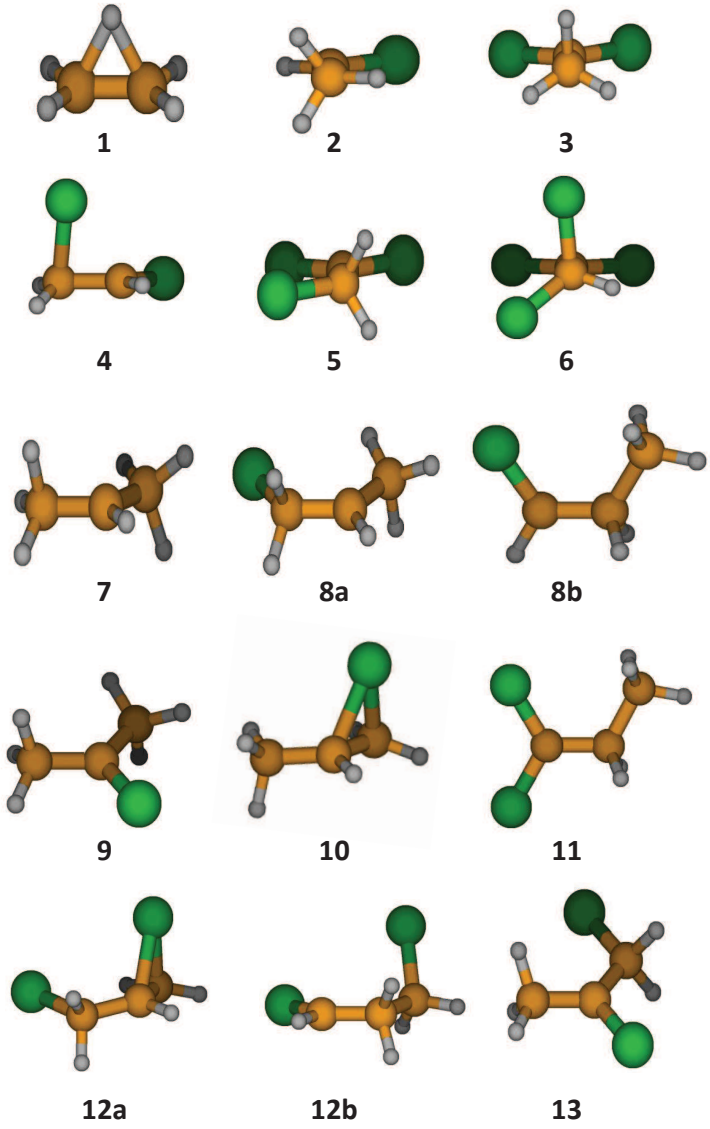

Figure 5.3: Structures of protonated ethenes and propenes predicted using G4. An overview of the parent molecules are given in Table 5.5. From Ref. [3].

presented in Fig. 5.3. For ethene (**1**), the stable protonated structure involves a bridging proton and the positive charge is delocalized over the entire molecule. The structures **2**, **3**, **5**, **8a**, **8b**, **9**, **11**, **12b**, and **13** can be classified as classic protonated structures. A sigma bond is formed between the added proton and carbon at the formal site of protonation with retention of all sigma bonds present in the accepting molecule. The positive charge is mostly localized to the geminal carbon. A sigma bond between the proton and the carbon is formed also in **10** and **12a**. In addition the remaining molecular framework is rearranged so that a terminal sigma-bonded chlorine is transferred to a bridging position to form a chloronium ion.[74] **4** and **6** may be considered semi-classical structures. **4** is not a pure bridging structure although the chlorine is bent towards the other carbon and in **6**, the protonated carbon is rotated so that the symmetry is broken. As will be shown, the final structure is important for the resulting protonation enthalpy.

5.2.1 Protonation enthalpies

Computed protonation enthalpies are presented in Tab. 5.5 together with previously published results. Experimental results are only available for ethene, propene, and 2-methylpropene and for these compounds, our computed results are 0.01 eV higher, 0.01 eV lower, and 0.1 eV higher, respectively. Concerning the general quality of G4, it has been tested against a set of 454 experimental energies, commonly referred to as the G3/05 test set.[79] Average absolute deviation from experiment is 0.83 kcal/mol (0.036 eV) for all the energies. For the 10 proton affinities included in the test set, the average absolute deviation is 0.84 kcal/mol (0.036 eV) and the root mean square deviation 1.04 kcal/mol (0.045 eV). Also taking into account that chlorine is a demanding substituent to model, we estimate the uncertainties for our computed results to be in the range of 2 kcal/mol (0.09 eV).

For the three dichloroethenes, our results are 0.12-0.19 eV higher than those reported by Frash *et al.* in Ref. [76]. In the same publication, computed protonation enthalpies for the di-fluorinated ethenes were found to be 0.26-0.56 eV lower than the experimental values. Assuming a similar trend for the dichlorinated ethenes, our results are closer to experimental values than those reported by Frash *et al.*

5.2.2 Substituent parameters for protonation

As for the ionization energies above, it is useful to discuss the protonation enthalpies in terms of substituent effects. For protonation, we define a substituent to be in α position if connected to the site of protonation and β if on the neighboring sp^2 carbon. For simplicity, we refer to a chlorine in α (β) position as an α (β) chlorine. The parameters are derived as shifts

Table 5.5: *Enthalpies of protonation (ΔH_{prot}) (eV).*

Molecule	Label	H^+on	ΔH_{prot}	Prev. published
Ethene	**1**		-7.06	-7.05[a], -7.09[b]
Chloroethene	**2**	C2	-7.44	
1,1-Dichloroethene	**3**	C2	-7.77	-7.63[c]
Cis-1,2-dichloroethene	**4**		-7.12	-6.93[c]
Trans-1,2-dichloroethene	**4**		-7.15	-7.03[c,d]
Trichloroethene	**5**	C2	-7.40	
Tetrachloroethene	**6**		-7.22	
Propene	**7**	C1	-7.72	-7.73[d], -7.94[b]
Cis-1-chloropropene	**8a**	C1	-7.25	
	8b	C2	-7.50	
Trans-1-chloropropene	**8a**	C1	-7.27	
	8b	C2	-7.52	
2-Chloropropene	**9**	C1	-8.01	
3-Chloropropene	**10**	C1	-7.74[e]	
1,1-Dichloropropene	**11**	C2	-7.79	
Cis-1,3-Dichloropropene	**12a**	C1	-7.42[e]	
	12b	C2	-7.33	
2,3-Dichloropropene	**13**	C1	-7.70	
2-Methylpropene		C1	-8.41	-8.31[a], -8.31[f]

[a] Experimental results, see Ref. [75].
[b] Computed results from Ref. [21].
[c] Computed results from Ref. [76].
[d] Experimental results, see Ref. [77].
[e] The protonated species are chlorine-bridged structures.
[f] Computed results from Ref. [78].

relative to ethene in a similar manner as described above for the ionization energies.[2] Except for 1-chloropropene and *cis*-1,3-dichloropropene, we are only able to protonate at one site. As a result, only β parameters can be obtained directly from the data. α parameters are computed as shifts assuming that the effect of the two substituents are additive. Tab. 5.6 summarizes the results of substituting hydrogen with chlorine or a methyl or chloromethyl group at the specified position.

We observe that a β chlorine decreases the protonation enthalpy by -0.39 eV while the corresponding value for methyl is -0.66 eV. A β chloromethyl group may cause a lowering of the protonation enthalpy by -0.26 eV. However, protonation of 3-chloropropene and C1 in *cis*-1,3-dichloropropene leads to structures with a bridging chlorine, and the effective lowering is then far larger, amounting to -0.69 eV. Common for all the β substituents is that they favor protonation relative to ethene. Further-

Table 5.6: *Substituent parameters for protonation enthalpies (eV). Values in parenthesis are obtained indirectly from the data assuming additivity.*

Substituent	Cl		CH_3		CH_2Cl	
Postition	α	β	α	β	α	β
ΔH	(0.32)	-0.39	(-0.04)	-0.66	(0.11)	-0.26[a]/-0.69[b]

[a] Non-bridging structure. [b] Bridging chlorine, chloronium ion.

more, the observed saturation effects for chlorine and methyl are small. The protonation enthalpy of C2 in 1,1-dichloroethene is only 0.06 eV lower than twice the difference between chloroethene and ethene. Similarly, the protonation enthalpy of 2-methylpropene is only 0.1 eV lower than twice the difference between ethene and propene.

When in α position, chlorine increases the protonation enthalpy by about 0.3 eV. Knowing that chlorine is strongly electron withdrawing, it is not surprising that a α chlorine makes the site less attractive for an electrophilic attack by a proton. The corresponding number for chloromethyl is about 0.11 eV and for methyl it is close to zero, although being slightly negative.

We can make use of the substituent parameters in Tab. 5.6 to explain the variations in protonation enthalpies observed in Tab. 5.5. As a chlorine in β position increases the protonation enthalpy more than a α chlorine decreases it, it is easier to protonate tetrachloroethene than 1,2-dichloroethene. Furthermore, among the chlorinated compounds, the most negative protonation enthalpy is found for C1 in 2-chloropropene. It has both chlorine and methyl in β position, both strongly reducing the protonation enthalpy. The total effect is only 0.1 eV lower than the sum of each substituent acting independently and again the substituent effect is small.

5.2.3 Π donation from chlorine upon protonation

From the changes in electrostatic potentials (ΔEKT) above,[2] we see that chlorine has a electron withdrawing effect also when in the β position, which should, if acting alone, increase the protonaton enthalpy. The observed decrease in protonation enthalpy is therefore probably caused by relaxation. Chlorine can donate electrons upon demand and the actual donation depends also on abilities of the acceptor.

In a study of ionization and protonation of fluorinated benzenes Carroll *et al.* find the π donation from fluorine to be larger upon protonation than ionization.[22] Furthermore, they conclude that the accepting ability is strongly enhanced if one hydrogen is located above and one below the molecular plane so as to form one molecular orbital of σ symmetry and one of π symmetry. Except for **1**,**4** and **6**, all protonated species have similar arrangements of hydrogens. Fig. 5.4 shows an example of such a π reminiscent molecular orbital for chloroethene protonated at C2. The orbital is extending over most of the molecule, allowing for an effective charge donation from the β chlorine to the site of protonation. For protonated tetrachloroethene (**6**) this is not a possibility, as it has only one hydrogen. However, the somewhat surprising rotated structure with one chlorine above and below the molecular plane may be related to chlorine playing a similar role.

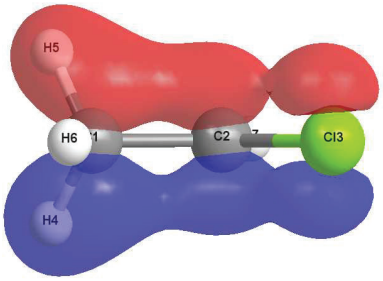

Figure 5.4: Example of π reminiscent molecular orbital for chloroethene. From Ref. [3].

5.3 Electrophilic addition of HCl

In the gas-phase, addition of HCl to a unsaturated carbon-carbon bond is a bimolecular reaction. As the transition-state species is extremely short-lived, it cannot be observed experimentally. However, computed geometries point towards a four-center state where the H-Cl and C-C bonds are partly broken whereas bonds between H and Cl and the two carbon atoms are partly formed, as shown for chloroethene in Fig. 5.5. The reaction is regiospecific and is classified either as Markovnikov or a anti-Markovnikov, depending on the orientation of HCl in the complex. In textbooks, Markovnikov addition is commonly defined as the addition where "the more highly substituted carbocation is formed as the intermediate rather than the less highly substituted one."[80] The definition refers to a situation where the reaction is carried out in solution. Then the reaction is likely to proceed in two steps: first the proton attacks the π bond and next, the chloride anion binds to the carbocation. In our case, we have a range of substituents (chlorine, methyl and chloromethyl) and it is sometimes difficult to decide which carbon is the most or least substituted. As a practical solution to this problem, we define the most stable carbocation as to the be most stable protonated species, as predicted by G4 in the previous section.

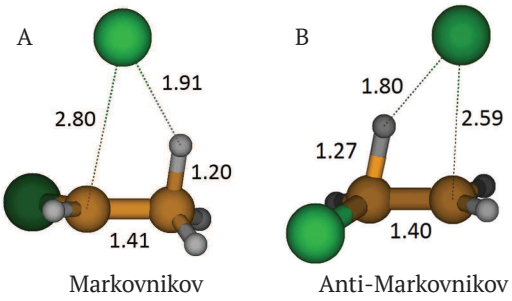

Figure 5.5: Electrophilic addition of HCl to chloroethene.

5.3.1 Activation energies

Activation energies (E_a) for the electrophilic addition of HCl are computed for the series of chlorinated ethenes and propenes described above, as well as for ethene and propene. Geometries for ground-state reactants and transition states are computed at the B3LYP/tzp level. Energies are computed using CCSD(T)/aug-TZ and basis set corrections (MP2/aug-QZ) and thermal corrections are included as described in Sec. 5.7. The energies are shown in Tab. 5.7 together with previously published results.

Experimental results are available only for ethene and propene and our computed results are 0.09 eV and 0.08 eV higher, respectively. However, neither of these compounds contain chlorine, and to better evaluate our computational routine, we also compute the activation energy for the elimination reaction of HCl from 1,1,1-trichloroethane and 1,1,1-trichloropropane. The resulting values of 56.3 and 55.3 kcal/mol can be compared to experimental results of 52 and 50 kcal/mol, as reported by Turpin *et al.* in Ref. [81]. It may therefore be assumed that our computed results for the chlorinated compounds overestimate the true activation energy by about 10%.

Table 5.7: *Activation energies (E_a) in the gas and solvent phase (eV).*

Molecule	H^+on	Orient.	$E_{a,gas}$	Prev.	$E^a_{a,solv}$
Ethene			1.81	1.72[b], 1.62[c], 1.78[d]	1.31
Chloroethene	C1	aM	2.09	2.10[e]	1.71
	C2	M	1.84	1.80[e]	1.22
1,1-Dichloroethene	C1	aM	2.29		2.02
	C2	M	1.90		1.17
Cis-1,2-dichloroethene			2.06		1.53
Trans-1,2-dichloroethene			2.08		1.50
Trichloroethene	C1	aM	2.23		1.80
	C2	M	2.10		1.45
Tetrachloroethene			2.24		1.69
Propene	C1	M	1.58	1.50[b], 1.36[c], 1.50[d]	0.92
	C2	aM	1.85	1.79[b], 1.69[c], 1.80[d]	1.33
Cis-1-chloropropene	C1	aM	1.84		1.32
	C2	M	1.91		1.32
2-Chloropropene	C1	M	1.66		0.97
	C2	aM	2.13		1.77
3-Chloropropene	C1	M	1.78		1.30
	C2	aM	1.88		1.51
1,1-Dichloropropene	C1	aM	2.03		1.63
	C2	M	1.96		1.28
Cis-1,3-Dichloropropene	C1	M	1.93		1.58
	C2	aM	1.89		1.39
2,3-Dichloropropene	C1	M	1.74		1.17
	C2	aM	2.14		1.83

[a] Solvent parameters defined by the keyword *1,1,1-trichloroethane*.
[b] Experimental results from Ref. [25].
[c] Computed results from Ref. [21].
[d] Energy computed at the CCSD(T)/cc-pVDZ level from Ref. [82].
[e] Computed results at the MP2/6-311+G(3df, 2p) level from Ref. [83].

5.3.2 Effects of a polarizable surrounding

Firstly, it should be emphasized that we have not performed true solvent state calculations as the applied Polarizable Continuum Model does not include any specific interactions between the solvent and the solute. However, the computations can be used to indicate the influence of a polarizable surrounding on geometries and energies, and we will for simplicity refer to the calculations as "solvent-state calculations", keeping the rather large limitations in mind.

Comparing geometries, we find that the transition state reminiscences more of a proton attack in the solvent state than in the gas phase. The hydrogen from HCl is more closely bonded to the molecule, whereas the HCl bond length and the C-H-Cl angle are increased.

The solvent-state and gas-phase E_a in Tab. 5.7 are predicted by two different methods and cannot be compared directly. However, gas-phase B3LYP/tzp energies were computed in the first step of optimization. Firstly,

as expected, E_a is lower in the solvent state compared to the gas phase as a polarizable surrounding will act to stabilize a localized charge. Interestingly, the average lowering in energy for the Markovnikov complexes is 0.34 eV whereas it is only 0.23 eV for the anti-Markovnikov ones. Comparing Mulliken charges, we find the Markovnikov complexes to have a higher dipole moment than the anti-Markovnikov ones, which is a plausible explanation why their stabilization energy is also higher.

5.3.3 Substituent parameters for E_a

To obtain a more detailed picture, we choose to investigate the influence of chlorine, methyl and chloromethyl in terms of substituent parameters (shifts relative to ethene) as described above for ionization and protonation. The two sets of E_a included in Tab. 5.7 are obtained by different methods and are therefore not directly comparable. We therefore include also substituent parameters based on gas-phase B3LYP/tzp calculations to be compared to the solvent-state parameters.

Table 5.8: *Substituent parameters for activation energies (eV).*

Substituent	Method	Cl		CH_3		CH_2Cl	
Position		α	β	α	β	α	β
Gas E_a	CCSD(T)[a]	0.28	0.03	0.04	-0.23	0.07	-0.03
Gas E_a	B3LYP/tzp	0.32	-0.02	0.07	-0.27	0.12	0.02
"Solvent" E_a [b]	B3LYP/tzp	0.40	-0.09	0.03	-0.38	0.21	-0.01

[a] CCSD(T)/aug-TZ with basis set corrections as described in the text.
[b] Using scrf solvent parameters for *1,1,1-trichloroethane*.

The first line in Tab. 5.8 describes the interaction parameters for our most accurate E_a computed using CCSD(T). An α chlorine causes a significant increase in E_a of 0.28 eV whereas a β chlorine has little influence. Methyl is on the other hand most important when in the β position and then lowers the activation barrier by 0.23 eV. Chloromethyl has a relatively small impact, the 0.07 eV increase from the α position being the most important. Both the α and β values fall between those of chlorine and methyl, as also observed for ionization and protonation.

The substituent parameters obtained when using B3LYP/tzp reproduce the results from CCSD(T)/aug-TZ within ± 0.05 eV. Going to the solvent phase, the most important contributions in the gas phase are enhanced whereas the smaller ones remain small. Noteworthy, β chlorine lowers the activation energy by about 0.1 eV in the solvent state, indicating that the accepting abilities are then enhanced, probably related to the larger ability of stabilizing a localized charge when in a polarizable surrounding. It is reasonable that this ability enhances both the withdrawing and donating

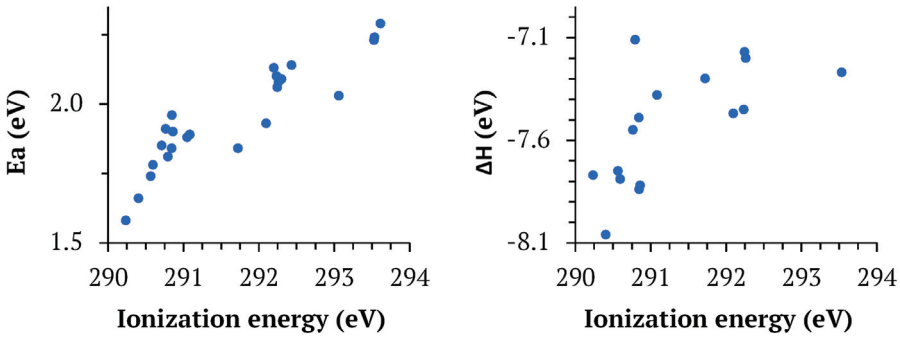

Figure 5.6: Activation energies (E_a) for electrophilic addition of HCl and protonation enthalpies (ΔH) and plotted against carbon 1s ionization energies.

abilities, as seen from the increased magnitude also for α chlorine, β methyl and α chloromethyl.

5.4 Ionization energies, protonation enthalpies and activation energies

In the previous sections, our results for measured ionization energies, computed protonation enthalpies, and computed activation energies for electrophilic addition of HCl are summarized. In the following sections, we compare the three processes and look for possible correlations between them. Fig. 5.6 shows computed gas-phase activation energies plotted against ionization energies to the left, and computed protonation enthalpies plotted against ionization energies to the right. In neither of the cases are there any clear correlation. The influences of chlorine, methyl and, chloromethyl in each of the three processes are already quantized in terms of substituent parameters and a comparison of the various substituent parameters may be a fruitful approach to explain the apparent lack of correlation. Next, we look at the data more in detail to see if there is a correlation between subsets of the data and if ionization energies may be used to predict protonation enthalpies and activation energies in these cases.

5.4.1 Ionization energies and activation energies

Tab. 5.9 includes the first-order interaction parameters for all the three processes ionization, protonation and electrophilic addition of HCl as derived in the preceding sections. Based on these, we can expect that for the chlorinated ethenes, gas-phase activation energies and ionization energies will correlate. For these molecules, we have only one substituent, namely chlo-

Table 5.9: *Substituent parameters for ionization energies, protonation enthalpies, and activation energies (eV).*

Substituent	Cl		CH_3		CH_2Cl	
Position	α	β	α	β	α	β
Ionization energy	1.51	0.05	-0.08	-0.56	0.22[a]	-0.27[a]
ΔH_{prot}[d]	(0.32)	-0.39	(-0.04)	-0.66	(0.11)	-0.26[b]/-0.69[c]
E_a, gas	0.28	0.03	0.04	-0.23	0.07	-0.03
E_a, solvent[e]	0.40	-0.09	0.03	-0.38	0.21	-0.01

[a]Average value for the conformers *syn* and *gauche*.
[b] Non-bridging structure. [c] Bridging structure.
[d]Values in parenthesis are obtained indirectly from the data.
[e]Using scrf solvent parameters for 1,1,1-trichloroethane.

rine. Since both processes have similar and negligible small β parameters, only the α parameter needs to be taken into account. Deterioration of the correlation is possible if the two processes have a very different pattern for saturation effects upon higher substitution. The linear fit to the gas-phase data (circles) in Fig. 5.7 has an R^2 of 0.97 and confirms that there is indeed a good correlation. However, going to the model of the solvent state (squares), the β parameters are 0.05 eV and -0.09 eV respectively, and the deteriorated correlation for the lower set of data is clearly related to this, as well as possible second-order effects. Except for the expected decrease in activation energy when going to the solvent state, there is a small increase in slope caused by the larger E_a α parameter for the solvent state compared to the gaseous state.

In Fig. 5.8 all activation energies for both the chlorinated ethenes and propenes are plotted against ionization energies. Holme *et al.* have studied the electrophilic addition of HCl to alkenes and alkynes and find a correlation between activation energies and ionization energies only for the Markovnikov additions.[26] We therefore separate between Markovnikov and anti-Markovnikov additions in the figure, keeping in mind the somewhat limited applicability of the definition of Markovnikov addition when more than one type of substituents are present. The data fall in three groups depending on the number of directly attached chlorines on the carbon. Those having no chlorines fall between 290 and 291 eV ionization energy, and those with one and two chlorines between 291.6-292.4 eV and 293-293.5 eV, respectively.

The lower, grey line represents the series of molecules having one β methyl and an increasing number of chlorines. As the slopes are dominated by the α chlorine effects, the slope of the lower line is fairly similar to that of the upper line, amounting to 0.16 and 0.15, respectively. The lower intercept is due to the β methyl parameters for E_a and IE both being negative. For the remaining points, deviations from ethene may roughly be explained with

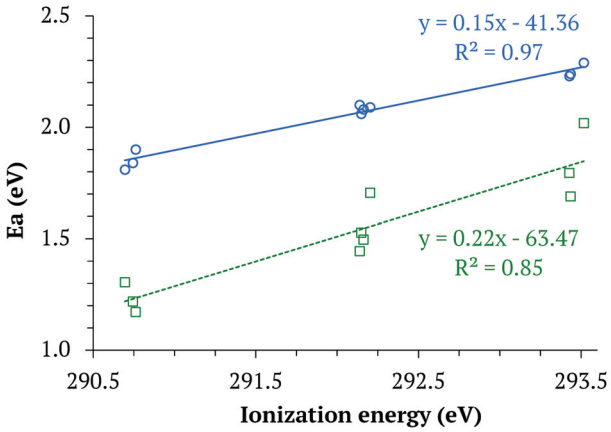

Figure 5.7: Gas-phase (circles) activation energies for addition of HCl plotted against ionization energies for the chlorinated ethenes. The squares represent activation energies when solvent effects are modeled as a polarizable surrounding.

similar arguments.

Three points dominated by the influence of α CH_2Cl fall close to the line. We may predict the slope of a line influenced by a certain substituent effect as the ratio between the substituent parameters. Hence, for an α CH_2Cl-line we would obtain 0.07/0.22=0.32. This is twice the slope of the fit to the gas-phase chloroethene data. However, since the two lines would have crossed in the middle of our plot, the three data points for CH_2Cl fall close to the fit for the chloroethene data. This example illustrates an important lesson, namely that apparent correlation cannot directly be taken as evidence for two phenomena being correlated. In fact, in the most extreme case, two different phenomena may seem to correlate simply if both have an additive behavior. Seemingly, an approach of comparing substituent effects is a more fruitful approach when more than one substituent is present or if a substituent contributes substantially both from an α and β position.

By using this approach, we are in the position to explain why Holme *et al* find a different correlation for the Markovnikov cases and anti-Markovnikov, as shown in the upper part of Fig. 9 in Ref. [26]. The α and β methyl parameters are -0.08 eV and -0.56 eV for ionization and 0.04 eV and -0.23 eV for electrophilic addition. Assuming that larger alkyl groups have similar parameters as methyl, we would to a first order predict Markovnikov addition to linear terminal alkenes to be influenced by β parameters, both being large and negative. Anti-Markovnikov additions would on the other hand only be influenced by α parameters. As α E_a is small but positive and α IE is negative, the points fall above the line that fits the Markovnikov

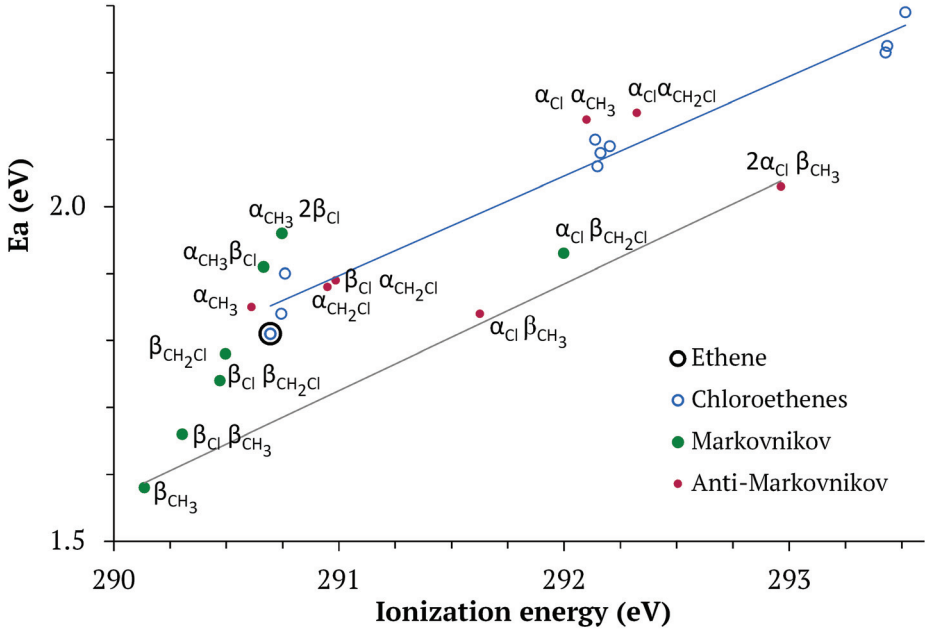

Figure 5.8: Gas phase activation energies for addition of HCl are plotted against ionization energies. Ethenes are marked with open circles and propenes with filled. For the propenes, green points correspond to Markovnikov and red to anti-Markovnikov addition. Ethene is marked with a black circle.

additions. Shifts for non-terminal alkenes would be dominated by large β parameters but also influenced by α parameters, causing the points to fall above the line only taking β contributions into account. Our predictions coincide with the observed pattern.

5.4.2 Ionization energies and protonation enthalpies

Gas-phase protonation enthalpies are plotted versus C1s ionization energies as shown in Fig. 5.9. Focusing on the chlorine substituent, the data are divided into subgroups depending on the number of α and β chlorine substituents, as indicated by the label (α, β), explained as (M,N) in the figure. The two non-chlorinated alkenes (0,0), ethene and propene, appear to the left. The second group is indicated with red circles and include five compounds having one β chlorine and no α chlorines and the fit to these points has a slope of 0.98. In addition to β chlorine, these also have α chloromethyl (**12b**), α methyl (**8b**), β chloromethyl (**13**), and β methyl (9). The correlation may seem promising at first glance. However, if this correlation was

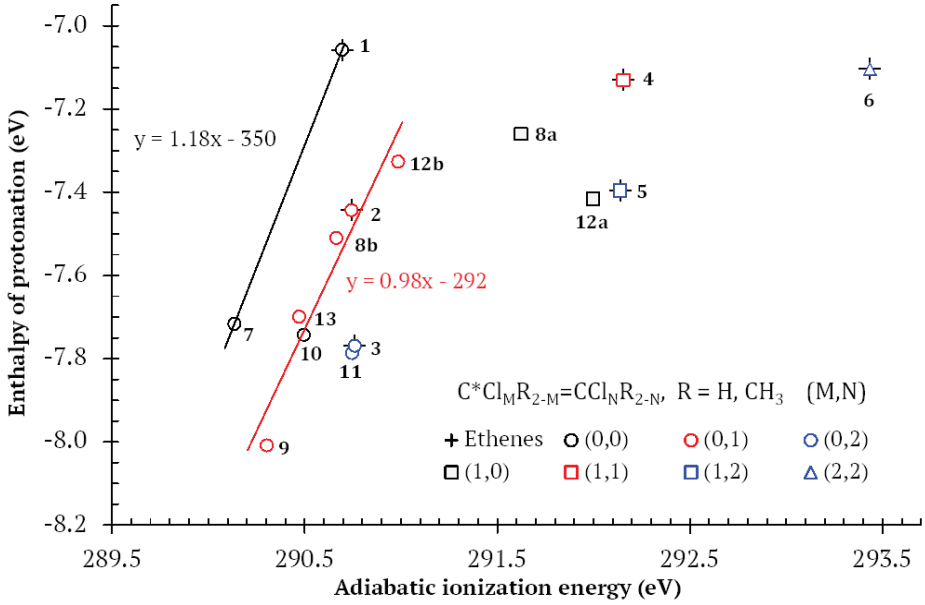

Figure 5.9: Proton affinities plotted versus ionization energies for chlorinated ethenes and propenes.

completely dominated by β chlorine contributions, we would have expected a different pattern, namely a line passing through **1** and **2** and with a slope close to -8, as obtained from the ratio of the β parameters for ionization and protonation. The corresponding ratia for the other substituents are all in the range 0.9-2, modifying the slope of the final fit to become positive. The small deviation in ratia between the non-chlorine substituents explain why we observe a correlation seemingly defined by the number of β chlorines.

5.4.3 Concluding remark

The important lesson from the foregoing comparisons is that a given group of substituents may or may not display a correlation with respect to two different processes. To interpret a pattern and also to predict when such correlations can be expected, we recommend the use of substituent parameters.

5.5 Computational accuracy

As already mentioned, chlorine was expected to be a demanding substituent to model accurately. Therefore, much effort has been devoted to establishing the level at which the computations had the necessary and desired accuracy,

both in terms of electronic-structure method and basis set. To this end, geometries and relative ionization energies are useful quantities as they can be compared to measurements. A full comparison of geometries would be too extensive and the C-Cl bond length was chosen for the comparison based on its importance when predicting vibrational lineshapes.[1]

5.5.1 Relative theoretical ionization energies

For the chlorinated ethenes and propenes, theoretical shifts in ionization energies were computed using six different combinations of electronic-structure methods and basis sets. [2] Tab. 5.10 summarizes the deviations when comparing to measured results. The largest mean error is found for CCSD(T)/tzp, amounting to 116 meV. Clearly the error is related to the basis set as changing to aug-TZ decreases it to 31 meV. This is further confirmed by comparing to B3LYP, which is less demanding with respect to basis set. Here tzp produces results within a mean absolute error of 65 meV. The overall large errors for MP2 indicate that it does not include the necessary level of correlation. MP4(SDQ) produces satisfactory accuracy with aug-TZ whereas the errors are actually larger for the aug-QZ basis. The lower part of Tab. 5.10 shows the resulting parameters when fitting measured shifts to the computed shifts. Correcting for systematic errors, we obtain chemical accuracy for CCSD(T)/aug-TZ and also MP4(SDQ) both using aug-TZ and aug-QZ. The best overall results are obtained using CCSD(T)/aug-TZ.

The shifts are computed using an effective core potential (ECP) to represent the core of the ionized carbon. The possible error related to this is explored by conducting proper hole-state calculations at the HF/aug-TZ level of theory. For the chlorinated ethenes, the errors are found to vary from 0 to 44 meV. This is higher than similar results for pure hydrocarbons, where the average errors are found to be less than 10 meV.[84] Hence, to compute shifts in ionization energies for chlorinated compounds with chemical accuracy, ECP-related errors should also be corrected for.

5.5.2 Geometries: C-Cl bond lengths

The chloromethane series was considered a proper testing ground for the accuracy of computed C-Cl bond lengths. [1] Firstly, Refs. [35] and [85] report measured ground state geometries of CH_3Cl, CH_2Cl_2, $CHCl_3$ and CCl_4 that may be compared to computed. Secondly, the theoretical Franck-Condon profile is highly dependent on the predicted change in geometry. To be able to reproduce the experimental spectrum well, the predicted changes in geometries need to be correct, and hence we may indirectly test also the final-state geometries. We describe our best model for computing changes in C-Cl bond lengths in the next section. Here, we summarize our results for computed ground-state bond lengths, cf. Tab. 5.11.

Table 5.10: *Comparison between measured and computed shifts in ionization energies for chloroethenes and chloropropenes. From Ref. [2].*

Comp. method	B3LYP	CCSD(T)		MP4(SDQ)		MP2
Basis	tzp	tzp	aug-TZ	aug-TZ	aug-QZ	aug-QZ
Errors compared to experimental results (meV)						
Mean error	53	116	18	31	41	82
Mean abs. error	65	117	31	31	50	99
RMSE	81	132	37	48	59	123
Max error	161	235	79	95	120	284
Measured ionization energies fitted to theoretical energies						
Slope	0.952(6)	0.955(7)	0.984(5)	0.975(4)	0.966(4)	0.927(8)
Intercept (meV)	-10(8)	-73(10)	-4(6)	-9(6)	-11(6)	-15(11)
RMSD (meV)	40	47	30	27	28	56

Generally, MP2 compute bond lengths that are too short while B3LYP bond lengths are too long. CCSD(T) has a slow convergence with basis set, as also found by Demaison and coworkers.[35] Core-valence correlations were computed at the MP2 level and the results were confirmed with test calculations using CCSD(T)/aug-TZ. Our best estimates amount to -0.0037 Åfor all four molecules. Basis set superposition errors where corrected for by means of counterpoise calculations. According to these results, the bond lengths are computed to be 0.4-0.6 pm too short when using aug-TZ and 0.2-0.3 pm for QZ. Our best estimates for the C-Cl bond lengths include geometry optimizations at the CCSD(T)/QZ level with core-valence and BSSE corrections. The resulting values fall between the two set of experimental results with differences of 0.6 pm or less. Hence, it seems more challenging to obtain chemical accuracy for geometries than for energies.

Table 5.11: *Ground-state C–Cl Bond Lengths (in Å) for Chlorinated Methanes. From Ref. [1].*

	Basis sets	CH_3Cl	CH_2Cl_2	$CHCl_3$	CCl_4
B3LYP	cc-pV(Q+d)Z	1.7942	1.7804	1.7661	1.7802
Valence-correlated optimizations					
MP2	(aug-)cc-pV(T+d)Z	1.7771	1.7649	1.7609	1.7645
MP2	cc-pV(Q+d)Z	1.7720	1.7601	1.7562	1.7598
MP4SDQ	tzp	1.8019	1.7870	1.7817	1.7850
CCSD(T)	tzp	1.8074	1.7920	1.7863	1.7893
CCSD(T)	(aug-)cc-pV(T+d)Z	1.7885	1.7748	1.7700	1.7733
CCSD(T)	cc-pV(Q+d)Z	1.7826	1.7692	1.7645	1.7677
CCSD(T)	pc-3	1.7818	1.7686	1.7641	1.7675
Core-valence corrections					
Best estimate [a]		-0.0037	-0.0037	-0.0037	-0.0037
Counterpoise corrections					
MP2	(aug-)cc-pV(T+d)Z	0.0063	0.0058	0.0051	0.0044
MP2	cc-pV(Q+d)Z	0.0032	0.0032	0.0026	0.0020
Corrected geometries					
CCSD(T)/(aug-)cc-pV(T+d)Z[b]		1.7911	1.7769	1.7714	1.7740
CCSD(T)/cc-pV(Q+d)Z[b,c]		1.7821	1.7687	1.7634	1.7660
Experimental [d]		1.7768(2)	1.766(2)	1.760(2)	1.767(2)
Experimental [e]		1.7854(10)	1.7724(20)	1.758(2)	1.7667(30)

[a] Prepared as the average for CH_3Cl and CH_2Cl_2 from CCSD(T)/(aug-)cc-pCV(T+d)Z and further corrected for basis-set incompleteness as MP2/cc-pCV(Q+d)Z - (MP2/(aug-)cc-pCV(T+d)Z).

[b] Corrected for core-valence correlation[a] and BSSE (MP2).

[c] Best estimate. [d] Demaison (2003), Ref. [35]. [e] Landolt-Börnstein, Ref. [85].

5.6 Lifetime of core holes in chlorinated methanes

Ref. [1] reports the measured C1s spectra of CH_3Cl, CH_2Cl_2, $CHCl_3$, and CCl_4. The spectra are fitted with the aim of predicting the vibrational lineshapes as accurately as possible. In Sec. 4.4, possible shortcomings to our usual procedure for computing Franck-Condon factors are outlined. To summarize, for the present series of molecules both Duschinsky effects and thermal excitations have a very small impact and can be neglected. Only a small improvement is observed when applying internal coordinates instead of Cartesian coordinates. The potential energy surface is well represented by a harmonic function for all modes except the symmetric C-H stretching mode at the core-ionized carbon. Hence, we focus in the following on obtaining an accurate description of changes in geometries upon ionization. To be more specific, we focus on the C-Cl bond contraction.

Geometries are optimized at the CCSD(T)/cc-pC*V(Q+d)Z level followed by a set of additional corrections. Basis set superposition errors are corrected for by means of counterpoise corrections computed at the MP2/cc-pV(Q+d)Z level. Due to canceling between the initial and final states, the corrections to the C-Cl bond are found to be small, between -0.02 and 0.02 pm. Core-valence correlation corrections computed at the MP2/cc-pCV(Q+d)Z level are about -0.1 pm, hence an overestimation of the contraction. The largest error is related to the core hole being described by an effective core potential (ECP). At the HF level of theory, this error is independent of basis set and amounts to -0.30(2) pm. This is of similar magnitude to the correction predicted for the contraction of the C-H bond in core-ionized methane and indicates that it is primarily depending on the ECP rather than the substituent.[61]

After assuring that the vibrational lineshapes have the necessary quality, they are convoluted with a Gaussian function to account for instrumental- and Doppler broadening. The instrumental broadening is constrained to be equal to the value obtained for CO_2 from the calibration spectrum. Also, the lineshape is convoluted with a combined function to account for post-collision interactions and lifetime broadening, as described in Sec. 4.3. The Lorentzian component is left as a free parameter and can then be determined in a fit to the spectrum. As can be seen in Fig. 5.10, the match to the experimental spectra is highly satisfactory. Based on these spectra, we conclude that the lifetime broadening values for the series of chlorinated methanes are 88±5 meV for CH_3Cl, 80±5 meV for CH_2Cl_2, 74±5 meV for $CHCl_3$ and 62±5 meV for CCl_4. They are all lower than the reported lifetime of methane, 95±5 meV.[71, 72]

In Fig. 5.11, our experimental lifetimes are compared to estimates obtained from a statistical model proposed by Walsh, Meehan, and Larkins.[86]

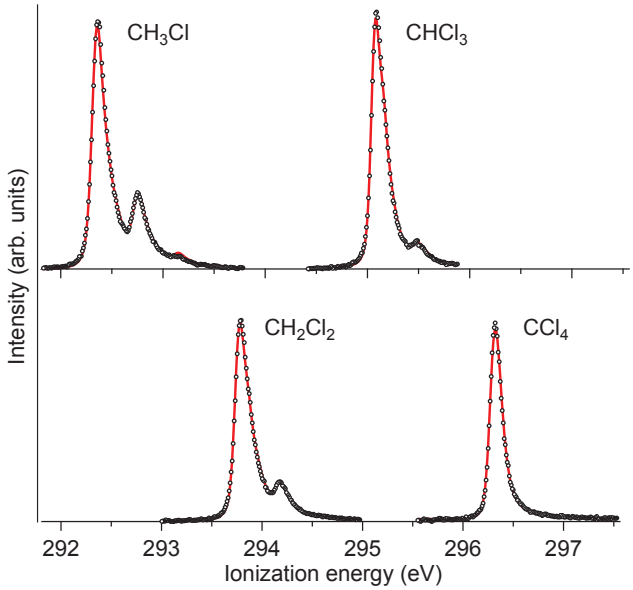

Figure 5.10: Carbon 1s spectra of the four chlorinated methanes (circles) fitted with theoretical lineshapes (red). The figure is reprinted from Ref. [1] with permission.

The model is based on an assumption that the Auger rates scales with the population in the valence orbitals. Predictions, as obtained from Eq. (3) in Ref. [86], are scaled to give a lifetime of 95 meV for methane. We obtain a squared correlation coefficient of 0.985, a slope of 1.055 and a constant term of -8 meV. The high degree of correlation between the two set of data indicate that the one-center model for Auger decay of the core hole is valid for the chlorinated methanes.

Furthermore, for the present compounds, there is a correlation between the core ionization energies and lifetime broadening, consistent with a hypothesis presented by Shaw and Thomas.[87] For the series of chlorinated methanes, the lifetime broadening is reduced by 5-6 meV per 1 eV increase in ionization energy.

5.7 Probing relative abundance of conformers by means of XPS

Both 3-chloropropene and 2,3-dichloropropene possess stable rotational conformers due to the hindered rotation of the terminal chloromethyl group. 3-Chloropropene exist as a *syn* conformer (Cl eclipsed with the C=C bond) and a *gauche* conformer (H eclipsed with the C=C bond). 2,3-

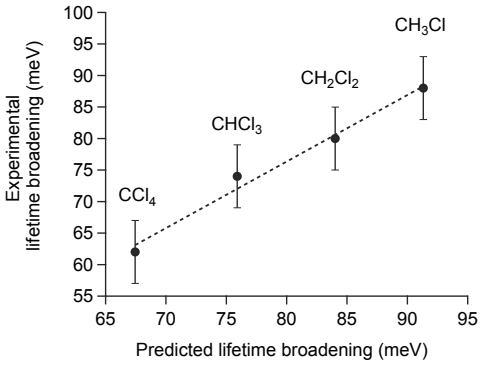

Figure 5.11: Comparison between experimental and predicted lifetime broadening in the chlorinated methanes. Reprinted from Ref. [2] with permission.

Dichloropropene can be either in an *anti* conformer (Cl-C3-C2-Cl=180 deg) or one of two *gauche* conformers (Cl-C3-C2-Cl=±71.2 deg). The spectra of 3-chloropropene and 2,3-dichloropropene are included in Fig. 5.12. Since the ionization is so fast, it provides an instant picture (snapshot) of the conformal situation in the molecule. As a result of this, the theoretical lineshapes need to be both site- and conformer specific and the spectra are fitted using six different theoretical lineshapes.

For several reasons, the prediction of lineshapes was a non-trivial task. Firstly, the presence of soft modes with significant thermal excitation in the ground state is in conflict with an assumption in our standard Franck-Condon analysis, namely that the molecule initially is in its vibrational ground state. Secondly, several of the propenes undergo large internal rotations upon ionization, severely weakening the foundation for a harmonic treatment of the corresponding vibration. The solutions to each of these problems are detailed in Ref. [2] (partly as Supplementary information) and are too extensive to be repeated here.

Equipped with conformer- and site-specific lineshapes, these are fitted to the experimental spectrum following the procedure described in Sec. 4.3. An additional constraint is imposed, namely that the ratio of each conformer should be similar for all sites. Hence, for 3-chloropropene, the constraint is: $\mathrm{C1}_{gauche}/\mathrm{C1}_{syn} = \mathrm{C2}_{gauche}/\mathrm{C2}_{syn} = \mathrm{C3}_{gauche}/\mathrm{C3}_{syn}$. As already mentioned, it is documented that the presence of chlorine often reduces the intensity of the carbon to which it is attached, leading to a non-stoichiometric behavior, and this constraint accounts for that. However, possible rotational-dependent long-range effects are not accounted for. The relative populations of each conformer were obtained from the intensities of the lineshapes. We find that the relative intensity of the *anti* conformer of 2,3-dichloropropene to be 52±8%. Trongmo *et al.* performed gas electron diffraction exper-

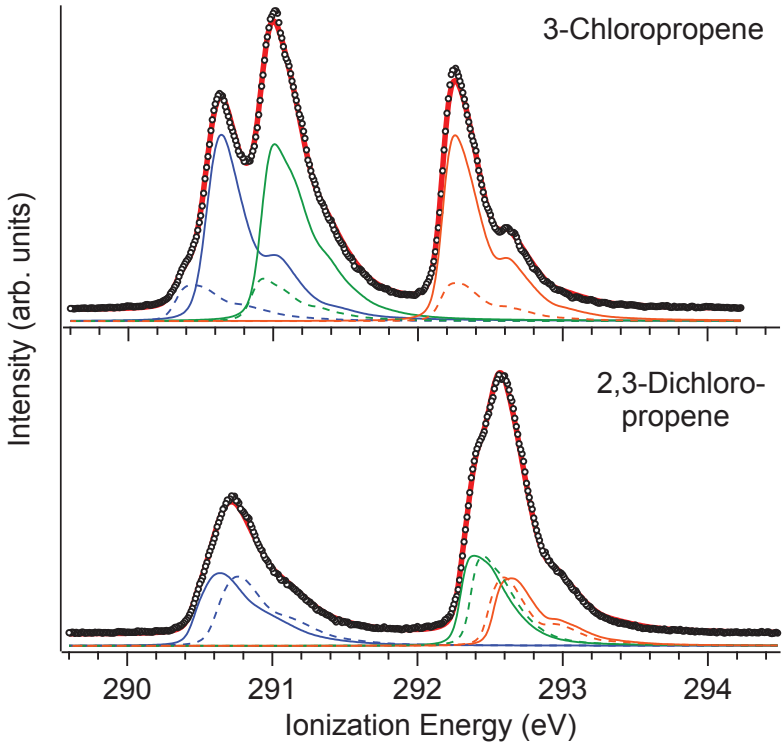

Figure 5.12: Carbon 1s photoelectron spectra of 3-chloropropene and 2,3-dichloropropene. The spectra were fitted using one theoretical profile for each chemically unique carbon [C1 (blue), C2 (green), and C3 (orange)] and for each conformer. The less stable conformers, 3-chloropropene *syn* and 2,3-dichloropropene *gauche*, are represented by dotted lines.

iments and found the corresponding number to be 55±8% at 24°C. The population of the *syn* conformer of 3-chloropropene is 18±8%. This is similar to the gas electron diffraction result of 18±9% reported by Schei *et al.*[88] Hence, given that site- and conformer-specific theoretical lineshapes can be predicted with sufficient accuracy at and least one of the sites have qualitatively different lineshapes for the two conformers, high-resolution XPS provides a reliable source for the determination of relative populations of conformers, as already established.[8, 11, 89, 90]

5.8 Adsorption of 1,1-dichloroethene to a Si(111)-7×7 surface

In two papers, we focus on the adsorption of 1,1-dichloroethene to the Si(111)-7×7 surface[4, 5] and the main results will be summarized in the

following sections. In addition, non-stoichiometric behavior of the CCl_2 carbons is discussed in light of more recent results.

5.8.1 Chemisorption

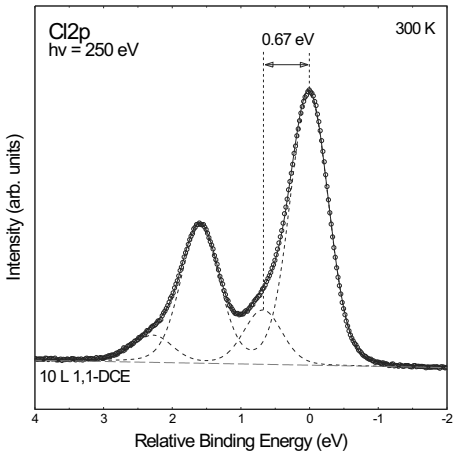

Figure 5.13: Chlorine 2p spectrum of 1,1-dichloroethene chemisorbed to Si(111)-7×7. The figure is reproduced with permission from Ref. [4].

Previous studies conclude, based on various spectroscopic techniques (conventional XPS, vibrational electron energy loss spectroscopy (EELS) and thermal desorption spectrometry (TDS)) [91–93], that the chemisorption is preferred to happen by breakage of either one or two carbon-chlorine bonds but also reveal a disagreement concerning which of these is preferred. The chemisorption of 1,1-dichloroethene is therefore studied by means of high-resolution XPS.[4]

In addition to carbon 1s spectra, also chlorine 2p spectra are measured, shown in Fig. 5.13. At least two different chemical components are present, each having a spin-orbit splitting. The main component covers 84% of the intensity and is at 0.67 eV lower energy than the minor peak covering 16%. By comparing the electronegativity of silicon (1.90) and carbon (2.55), it is concluded that the main component can be assigned to chlorine atoms bonded directly to silicon while the smaller contribution correspond to chlorine bonded to carbon. Assuming that the intensities correspond to the relative stoichiometry, it follows from these observations that, at room temperature, 1/3 of the molecules are single-bonded to the silicon surface (Si(111)–ClC=CH_2), while 2/3 are double bonded (Si(111)>C=CH_2).

C1s spectra are measured at photon energies (hν) of 320 and 330 eV and the spectra are shown in Fig. 5.14. Interpretation of these spectra is less clear cut since at least five components (**a-e**) are present. Therefore,

Table 5.12: *Theoretical and experimental shifts in C1s ionization energies relative to $=CH_2$ (eV).*

Theory [1]	Model	C bonded to Si	$=CH_2$
	$(SiH_3)_2C=CH_2$	-0.58	0.00
	$(SiH_3)ClC=CH_2$	1.24	0.13
	$(SiH_3)_4C$	-1.16	
	$(SiH_3)HC=CH(SiH_3)$	-0.36	
Experiment	$h\nu$ = 330 eV (320 eV)[2]	C bonded to Si	$=CH_2$
	Si(111)>C=CH_2	**d**: -0.48 (-0.45)	**c**: 0.00
	Si(111)–ClC=CH_2	**a**: 1.36 (1.31)	**b**: 0.44 (0.40)
	Si–C	**e**: -1.12 (-1.09)	

[1] Calculated shifts are scaled with a factor of 0.915, a factor taken from the difference between the calculated and experimental gas phase shift between the two peaks of 1,1-dichloroethene [2]. The energies are calculated relative to CH_2 in $(SiH_3)_2C=CH_2$. [2] Values obtained at $h\nu$ = 320 eV are shown in parentheses. The table is reprinted with permission from Ref. [4].

theoretical ionization energies are predicted for simple model compounds in an analogous manner as described above for the gas-phase compounds. The effect of silicon on the ionization energy is modeled by means of SiH_3 groups attached to carbon and computed results are shown together with measured relative ionization energies in Tab. 5.12. When modeling the attachment to the silicon surface more in detail, the most commonly used model is a Si_9H_{12} cluster.[28] However, the purpose of the present calculations is to obtain chemical shifts, which are usually dominated by the nearest neighbors. Note that possibility that various binding sites at a Si(111)-7×7 surface can have significantly different electronic properties is not accounted for. However, despite the rough quality of the model, it was able to reproduce the measured shifts within a reasonable range.

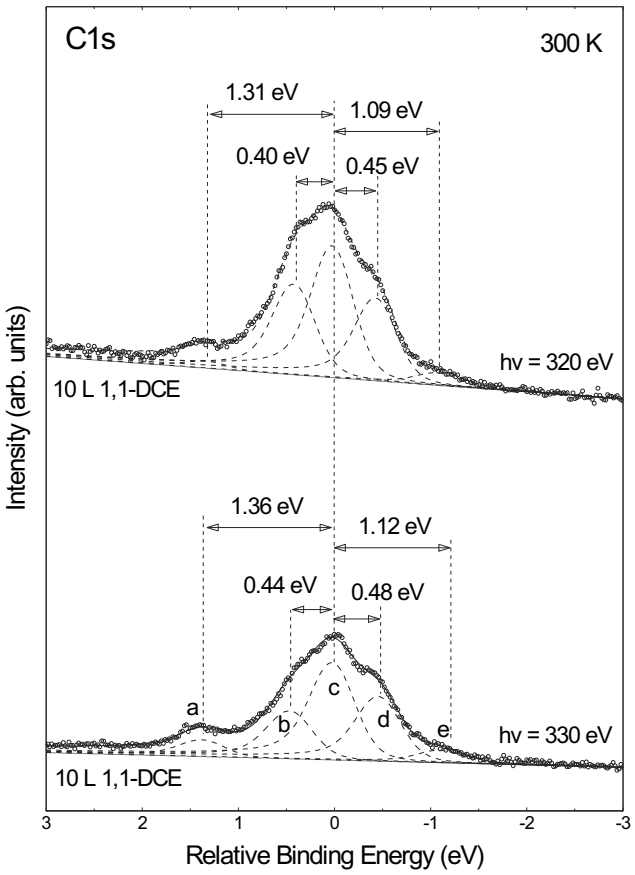

Figure 5.14: Carbon 1s spectra (open circles) measured after exposure to 10 L 1,1-DCE at 300 K followed by cooling to 120 K. The lower spectrum is measured with a photon energy of 330 eV, the upper spectrum with a photon energy of 320 eV. The dashed lines show the different contributions to the each of the spectra and the solid lines the overall fit. The identity and chemical shifts of components **a**, **b**, **c**, **d**, and **e** are explained in Tab. 5.12. The figure is reproduced with permission from Ref. [4].

Based on the theoretical calculations, two peaks are assigned to the two $=CH_2$ moieties, namely the one originating from Si(111)>C=CH_2 (**c**) and the one originating from Si(111)-ClC=CH_2 (**b**). Based on the relative intensitites of these two peaks in the spectra measured at hν=330 eV it is found that 67% of the molecules break both C-Cl bonds when chemisorbing. The corresponding number for the spectra measured at hν=320 eV is 59%. Despite these deviations, the results are reasonably consistent with those based on the Cl2p spectra and we conclude therefore that 1/3 of the molecules chemisorb to the surface by breaking one C-Cl bond and 2/3 by breaking two bonds. There is a possibility that time, or also a local heating caused by radiation, can increase the proportion of double-bonded species, Si(111)>C=CH_2.

5.8.2 Physisorption

Fig. 5.15 displays the C1s photoelectron spectrum of 1,1-dichloroethene in the gas phase (A) and in the adsorbed state (B). The two peaks in the gas-phase spectrum are well separated. Also, they have significanly different peak shapes. The low-energy peak has a shoulder at 0.4 eV higher energy corresponding to the symmetric C-H stretching vibration of an ionized carbon. The high-energy peak is dominated by softer vibrations and has therefore a narrower shape. From the theoretical analysis, we know that the C-Cl stretching vibrations are much excited when ionizing C1. We can therefore unambiguously assign the low-energy peak to C2(CH_2) and the high-energy peak to C1 (CCl_2). The difference in vertical ionization energy between the two peaks, e.g. the difference in mean position, is 2.57±0.01 eV. Please note that Ref. [5] reports an erroneous value for this shift, as also commented in Ref. [2]. Due to a technical error, the vertical ionization energy of C2 was reported to be slightly too low, causing an overestimation of the shift. The correct vertical ionization energy for C2 is 290.99(3) eV.

The lower spectrum in Fig. 5.15 arise from 10 L physisorbed 1,1-dichloroethene on top of 10 L chemisorbed molecules. As for the chemisorption spectrum in Fig. 5.14, the spectrum is plotted on a relative energy scale and the center of the C1 peak is chosen as reference. The experimental spectrum (circles) has two distinct peaks and the low-energy peak also has a shoulder towards lower binding energy. It is fitted by three contributions, the first at low energy being the experimental chemisorption spectrum described above and reported in Ref. [4]. In addition, the two theoretical lineshapes predicted for gaseous 1,1-dichloroethene are used. The Gaussian widths of the two latter are allowed to vary in a least-squares fit to the data, resulting in a total fwhm of 0.85±0.03 eV for the C1 peak. To estimate the component caused by the physisorption, the estimated instrumental broadening is subtracted from the total broadening of each peak. The broadening caused by physisorption is found to be 0.70 eV for the same peak and is hence

the dominating component of the total broadening. Ref. [5] also includes a closer analysis of the origin of this extra broadening and concludes that it is caused by a distribution of ionization energies within each layer and also across the multilayer condensate.

Although difficult to observe simply by visual inspection, the two theoretical lineshapes are qualitatively different even when additional broadening is included. If they are interchanged, there is a significant increase in χ^2, the parameter monitoring the quality of the least-squares fit. The correct shift in vertical ionization energy between the two peaks is 2.59±0.03 eV, e.g. similar to the gas-phase shift within the error bars. Note that this is 0.09 eV lower than reported in Ref. [5] and is caused by the same error described above for the gas-phase shift. McFeely *et al.* compare the vertical ionization energy shifts of chloroethane in the gaseous state and physisorbed to a hydrogenated Si(111) and find the shift to be reduced by 0.02 eV in the physisorbed state compared to the gaseous state, less than the error limits of each experiment.[33] In both cases, there are relatively small changes.

Hence, for 1,1-dichloroethene physisorbed on Si(111)-7×7, both peak shapes and internal shifts in ionization energies correspond very well to the gas-phase spectrum. If extra Gaussian broadening is included, the gas-phase spectrum provides an excellent model of the physisorption spectrum. In fact, Ref. [5] also reports a similar investigation of 1,3-cyclohexadiene adsorbed on Si(111)-7×7. Based on the high capability of the model to reproduce the physisorption spectrum, we strongly suggest that gas-phase spectra are used on a routine basis when assigning physisorption spectra. This may be considered a further simplification of what is presented above, where theoretical lineshapes were used. If the gas-phase spectra are measured in advance, they may also be used during measurement to decide whether true physisorption is actually taking place under the chosen experimental conditions.

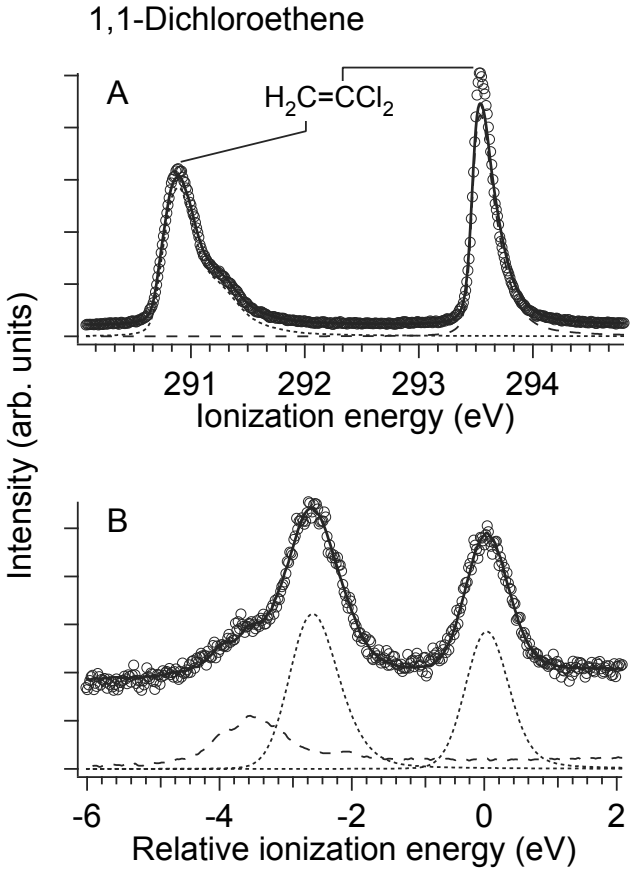

Figure 5.15: A) C1s photoelectron spectrum of gaseous 1,1-dichloroethene (circles). The overall fit (solid line) is the sum of two atom-specific theoretical lineshapes (dotted lines), one for each inequivalent carbon. B) C1s photoelectron spectrum of 1,1-dichloroethene adsorbed on a Si(111)-7×7 surface. The experimental spectrum (circles) contains contributions from both chemisorbed and physisorbed molecules. The overall fit (solid line) is a sum of theoretical lineshapes, one for each of the two carbons in the physisorbed layer (thin solid lines), and the experimental C1s chemisorption spectrum (broken lines). Reproduced with permission from Ref. [5]. © 2010 American Chemical Society.

5.8.3 On non-stoichiometric behavior

Both Ref. [4] and [5] comment that the C1s spectra reveal a non-stoichiometric behavior of the two carbons in the initial 1,1-dichloroethene. In the gas phase, the intensity of the C1 peak is 89% of that of C2 and the number is further reduced to 79% in the physisorbed state. In the chemisorbed state, the carbons bonded to silicone or chlorine have a significantly lower intensity than those bonded to hydrogen. More recent studies provide an explanation for this behavior. Söderström *et al.* report on large variations in relative stoichiometry between the two carbons in mono-, di-, and tri-chlorosubstituted ethane.[39] They find that the ratios have photon-energy dependent oscillations and that the amplitudes increase with increasing chlorine substitution. The oscillations can largely be predicted by means of theory used to interpret extended X-ray-absorption fine structure spectra (EXAFS). They conclude that the oscillations are caused by back-scattering from the chlorine atoms and also that the polarizability of the chlorine substituents leads to a higher probability of shake-up and shake-off. Carroll *et al.* report on a similar oscillating behavior for 2-butyne, even if this compound does not have any high-Z scattering center.[7] Our choice of photon energy is in the regions where the amplitudes are the largest and it is therefore likely that our spectra are influenced both by the oscillating scattering effects and the more constant difference caused by shake up/shake off and that this is the plausible explanation for the observed non-stoichiometric behavior. The optimized structure of the dimer of 1,1-dichloroethene reveals that the shortest intermolecular distance is between the two CCl_2 carbons. It is therefore reasonable that the scattering effects may be enhanced in the physisorbed state compared to the gas phase.

Chapter 6

Conclusions

We investigate chlorine as a substituent in 17 different chlorinated compounds. To be more specific, these include four chlorinated methanes, six chlorinated ethenes and seven chlorinated propenes.[1–5] In particular, we study the processes of carbon 1s ionization, protonation and electrophilic addition of HCl and we observe chlorine in a diversity of roles.

By comparing ionization energies for chlorinated ethenes and methanes relative to their non-chlorinated origins, we find that chlorine increases the ionization energy of the carbon to which it is attached by about 1.5 eV for chlorinated ethenes and propenes and 1.6 eV for the chlorinated methanes. When adding a second chlorine to the same carbon, a small saturation effect of about 0.2 eV is observed. We find that the most important contributions to the ionization energies come from the influence of chlorine on the ground-state potential, demonstrating the strong electron-withdrawing abilities of chlorine. Chlorine also contributes to the relaxation upon ionization through donation of electrons via the σ bond to the nearest neighbor and via the π bond to the second-nearest neighbor. We find that this π donation is remarkably enhanced upon protonation compared to ionization. The plausible explanation is that this increased donation is not only related to chlorine itself but also to the protonated site which is a better electron acceptor than an ionized site. Two hydrogens located above and below the molecular plane participate in a molecular orbital extending over most of the molecule, allowing for an effective charge donation from chlorine to the second-nearest carbon. An even more efficient charge donation is observed upon protonation of 3-chloropropene and 1,3-dichloropropene. In these cases the protonated species rearranges into a chloronium ion with chlorine in a bridging position, increasing the oxidation number of chlorine to +I. Upon electrophilic addition of HCl, chlorine primarily influences the nearest neighbor by increasing the activation energy by about 0.3 eV relative to ethene. The influence on the second-nearest neighbor is however negligible.

The core hole created upon ionization has a finite lifetime leading to an

uncertainty of the energy of the peak, referred to as lifetime broadening. The lifetime broadening values for the series of chlorinated methanes are determined from their carbon 1s spectra, and the resulting values are 88±5 meV for CH_3Cl, 80±5 meV for CH_2Cl_2, 74±5 meV for $CHCl_3$ and 62±5 meV for CCl_4. Comparison to a statistical model proposed by Larkins and coworkers indicate that a one-center model for Auger decay is valid for this series and that the electron withdrawing properties of chlorine increase the lifetime of a core hole on a neighboring carbon.

If chlorine is attached to the terminal sp^3 carbon in a propene, it may cause rotational isomerism, as observed for 3-chloropropene and 2,3-dichloropropene. Based on the relative intensities of the conformer- and site-specific vibrational lineshapes for these two compounds, we obtain a *syn* population for 3-chloropropene of 18±8% and an *anti* population for 2,3-dichloroethene of 52±8%, in close agreement with results obtained by electron diffraction measurements.

When chemisorbing 1,1-dichloroethene to a Si(111)-7×7 surface, we observe a surface-analog to a nucleophilic substitution reaction. C-Cl bonds are broken, and new bonds between carbon and the surface are formed. We find that 1/3 of the molecules bind by breaking one bond and 2/3 by breaking two bonds. Furthermore, as the carbon 1s shifts between chlorinated and non-chlorinated carbons are large, the spectrum of physisorbed 1,1-dichloroethene provides an excellent testing ground for comparison with the gas-phase spectrum. Based on the analysis, we recommend gas-phase carbon 1s spectra to be used on a routine basis when interpreting spectra of physisorbed species.

Chapter 7

Suggestions for further work

We have quantized the influence of chlorine, chloromethyl and methyl on ionization energies, protonation enthalpies and activation energies for electrophilic additions. However, we sought also to give a more qualitatively description of these influences and have only partly succeeded. On the theoretical side, a more detailed description of how electrons are transferred in each process would give a much better understanding of which properties of chlorine are the most important in each case and thereby also increase the predictability when extending to larger systems. Indeed, an analysis of electron donations upon ionization is included in Ref. [2]. An analysis of chlorinated ethanes and propanes, e.g. the saturated analogs of the compounds in the present study, could possibly allow us to separate the charge donation via the σ system to that of the π system.

When analyzing the spectra of the chlorinated methanes, correction parameters for the bond length of C-Cl were established with the aim to use these for larger systems, such as the chlorinated ethenes and propenes. Indeed, these corrections were useful for the cases of chlorinated ethanes.[6] However, going to sp^2 hybridized carbons in the ethenes and propenes, test calculations indicated these parameters were not valid anymore and a similar investigation would have to be done again if one would aim for the same accuracy in the fits.

Appendix A

List of abbreviations

Tab. 3.1 lists the common abbreviations used throughout the text. For abbreviations related to basis sets, please confer Tab. 3.1 at p. 17.

Abbreviation	Explanation
B3LYP	Becke-3-parameter exchange with LYP (Lee, Yang and Parr) correlation functional, cf. p. 15
BSSE	Basis-set superposition errors, cf. p. 18.
C*	Ionized carbon
C1, C2, ...	Carbon 1, 2, ... according to IUPAC nomenclature
C1s	Carbon 1s
Cl2p	Chlorine 2p
CCSD(T)	Coupled clusters with singles and doubles and perturbative triples, cf. p. 14.
DFT	Density functional theory, cf. p. 15.
E_a	Activation energy, cf. p. 19.
ECP	Effective core potential [60], cf. p. 18.
EKT	Extended Koopman's theorem [64], cf. p. 18.
FC	Franck-Condon, cf. p. 22.
fwhm	Full-Width at Half-Maximum.
ΔH_{prot}	Enthalpy of protonation.
HF	Hartree-Fock, cf. p. 14.
IE	Ionization energy
MP2	Møller-Plesset with double substitutions, cf. p. 14.
MP4(SDQ)	Møller-Plesset with single, double and quadruple substitutions, cf. p. 14.
scrf	Self consistent reaction field, cf. p. 19.
XPS	X-ray photoelectron spectroscopy

Table A.1: List of abbreviations used in the present work.

Bibliography

[1] M. G. Zahl, K. J. Børve, and L. J. Sæthre. Carbon 1s photoelectron spectroscopy of the chlorinated methanes: Lifetimes and accurate vibrational lineshape models. J. Electron Spectrosc. Relat. Phenom., 185: 226–233, 2012.

[2] M. G. Zahl, R. Fossheim, K. J. Børve, L. J. Sæthre, and T. D. Thomas. Electronic properties of chlorine as substituent to the ethylenic group – Viewed from the core of carbon. In manuscript, .

[3] M. G. Zahl, L. J. Sæthre, K. J. Børve, and T. D. Thomas. Proton affinity as predictor for electrophilic addition of HCl to chlorinated ethenes and propenes – A critical assessment. In manuscript, .

[4] T. H. Andersen, M. G. Zahl, I.-H. Svenum, K. J. Børve, A. Borg, and L. J. Sæthre. Chemisorption of 1,1-dichloroethene on the Si(111)-7×7 surface. Surf. Sci., 601:5510–5514, 2007.

[5] M. G. Zahl, V. Myrseth, T. H. Andersen, J. Harnes, A. Borg, L. J. Sæthre, and K. J. Børve. Molecular spectra as a tool in assigning carbon 1s photoelectron spectra of physisorbed overlayers. J. Phys. Chem. C, 114:15383–15393, 2010.

[6] M. Patanen, O. Travnikova, M. G. Zahl, J. Söderström, P. Decleva, T. D. Thomas, S. Svensson, N. Martensson, K. J. Børve, L. J. Sæthre, and C. Miron. Laboratory-frame electron angular distributions: Probing the chemical environment through intramolecular electron scattering. Phys. Rev. A, 87:063420–1–7, 2013.

[7] T. X. Carroll, M. G. Zahl, K. J. Børve, L. J. Sæthre, P. Decleva, A. Ponzi, J. J. Kas, F. D. Vila, J. J. Rehr, and T. D. Thomas. Intensity oscillations in the carbon 1s ionization cross sections of 2-butyne. J. Chem. Phys., 138:234310–1–5, 2013.

[8] A. Holme, K. J. Børve, L. J. Sæthre, and T. D. Thomas. Conformations and CH/π interactions in aliphatic alkynes and alkenes. J. Phys. Chem. A, 117:2007–2019, 2013.

[9] A. Berndtsson, E. Basilier, U. Gelius, J. Hedman, M. Klasson, R. Nilsson, C. Nordling, and S. Svensson. Ethene and chloroethenes studied by ESCA. Phys. Scripta, 12:235–247, 1975.

[10] T. X. Carroll, J. D. Bozek, E. Kukk, V. Myrseth, L. J. Sæthre, and T. D. Thomas. Line shape and lifetime in argon 2p electron spectroscopy. J. Electron Spectrosc. Relat. Phenom., 120:67–76, 2001.

[11] T. D. Thomas, L. J. Sæthre, and K. J. Børve. Effects of molecular conformation on inner-shell ionization energies. Phys. Chem. Chem. Phys., 9:719–724, 2007.

[12] R. L. Martin and D. A. Shirley. The relation of core-level binding energy shifts to proton affinity and Lewis basicity. J. Am. Chem. Soc., 96:5299–5304, 1974.

[13] D. W. Davis and J. W. Rabalais. Model for proton affinities and inner-shell electron binding energies based on the Hellmann-Feynman theorem. J. Am. Chem. Soc., 96:5305–5310, 1974.

[14] T. X. Carroll, S. R. Smith, and T. D. Thomas. Correlation between proton affinity and core-electron ionization potentials for double-bonded oxygen. Site of protonation in esters. J. Am. Chem. Soc., 97:659–660, 1975.

[15] B. E. Mills, R. L. Martin, and D. A. Shirley. Further studies of the core binding energy-proton affinity correlation in molecules. J. Am. Chem. Soc., 98:2380–2385, 1976.

[16] F. M. Benoit and A. G. Harrison. Predictive value of proton affinity. Ionization energy correlations involving oxygenated molecules. J. Am. Chem. Soc., 99:3980–3984, 1977.

[17] R. G. Cavell and D. A. Allison. Site of protonation in aromatic and acyclic amines and acyclic amides revealed by N1s core level electron spectroscopy. J. Am. Chem. Soc.99, 99:4203–4204, 1977.

[18] S. R. Smith and T. D. Thomas. Acidities and basicities of carboxylic acids. Correlations between core-ionization energies, proton affinities, and gas-phase acidities. J. Am. Chem. Soc., 100:5459–5466, 1978.

[19] R. S. Brown and A. Tse. Determination of circumstances under which the correlation of core binding energy and gas-phase basicity or proton affinity breaks down. J. Am. Chem. Soc., 102:5222–5226, 1980.

[20] D. Nordfors, N. Mårtensson, and H. Ågren. A critical investigation of XPS predicted proton affinities. J. Electron Spectrosc. Relat. Phenom., 56:167–187, 1991.

[21] T. D. Thomas, L. J. Sæthre, K. J. Børve, M. Gundersen, and E. Kukk. Reactivity and core-ionization energies in conjugated dienes. Carbon 1s photoelectron spectroscopy of 1,3-pentadiene. J. Phys. Chem. A, 109: 5085–5092, 2005.

[22] T. X. Carroll, T. D. Thomas, H. Bergersen, K. J. Børve, and L. J. Sæthre. Fluorine as a π donor. Carbon 1s photoelectron spectroscopy and proton affinities of fluorobenzenes. J. Org. Chem., 71:1961–1968, 2006.

[23] V. Myrseth, L. J. Sæthre, K. J. Børve, and T. D. Thomas. The substituent effect of the methyl group. Carbon 1s ionization energies, proton affinities, and reactivities of the methylbenzenes. J. Org. Chem., 72:5715–5723, 2007.

[24] T. X. Carroll, T. D. Thomas, L. J. Sæthre, and K. J. Børve. Additivity of substituent effects. Core-ionization energies and substituent effects in fluoromethylbenzenes. J. Phys. Chem. A, 113:3481–3490, 2009.

[25] L. J. Sæthre, T. D. Thomas, and S. Svensson. Markovnikov addition to alkenes. A different view from core-electron spectroscopy and theory. J. Chem. Soc., Perkin Trans. 2, pages 749–755, 1997.

[26] A. Holme, L. J. Sæthre, K. J. Børve, and T. D. Thomas. Chemical reactivity of alkenes and alkynes as seen from activation energies, enthalpies of protonation, and carbon 1s ionization energies. J. Org. Chem., 77: 10105–10117, 2012.

[27] K. Takayanagi, Y. Tanishiro, S. Takahashi, and M. Takahashi. Structure analysis of Si(111)7×7 reconstructed surface by transmission electron diffraction. Surf. Sci., 164:367–392, 1985.

[28] T. R. Leftwich and A V. Teplyakov. Chemical manipulation of multifunctional hydrocarbons on silicon surfaces. Surf. Sci. Rep., 63:1–71, 2008.

[29] A. Fink, W. Widdra, W. Wurth, C. Keller, M. Stichler, A. Achleitner, G. Comelli, S. Lizzit, A. Baraldi, and D. Menzel. Core-level spectroscopy of hydrocarbons adsorbed on Si(100)-2×1: A systematic comparison. Phys. Rev. B, 64:045308–1–9, 2001.

[30] F. D'Amico, R. Gunnella, M. Shimomura, T. Abukawa, and S. Kono. Dependence on the deposition conditions in the adsorption of C_6H_8 molecules on a Si(100)-2×1 surface. Phys. Rev. B, 76:165315–1–8, 2007.

[31] R. Gunnella, M. Shimomura, F. D'Amico, T. Abukawa, and S. Kono. Photoelectron diffraction of C_6H_8/Si(001): A model case for photoe-

mission study of organic molecules adsorbed on silicon surfaces. Phys. Rev. B, 73:235435–1–7, 2006.

[32] C. Papp, R. Denecke, and H. P. Steinrück. Adsorption and reaction of cyclohexene on a Ni(111) surface. Langmuir, 23:5541–5547, 2007.

[33] F. R. McFeely, K. Z. Zhang, and M. M. Banaszak Holl. Chloroethane physisorbed on hydrogenated Si(111): a test system for the evaluation of core level XPS assignment rules at Si/SiO_2 interfaces. Amorphous and Crystalline Insulating Thin Films - 199. Symposium, pages 15–20, 1997.

[34] H. Öström, L. Triguero, K. Weiss, H. Ogasawara, M. G. Garnier, D. Nordlund, M. Nyberg, L. G. M. Pettersson, and A. Nilsson. Orbital rehybridization in n-octane adsorbed on Cu(110). J. Chem. Phys., 118: 3782–3789, 2003.

[35] J. Demaison, L. Margulès, and J. E. Boggs. The equilibrium C-Cl, C-Br, and C-I bond lengths from *ab initio* calculations, microwave and infrared spectroscopies, and empirical correlations. Struct. Chem., 14: 159–174, 2003.

[36] M. Bässler, J.-O. Forsell, O. Björneholm, R. Feifel, M. Jurvansuu, S. Aksela, S. Sundin, S. L. Sorensen, R. Nyholm, A. Ausmees, and S. Svensson. Soft X-ray undulator beam line I411 at MAX-II for gases, liquids and solid samples. J. Electron Spectrosc. Relat. Phenom., 101-103:953–957, 1999.

[37] M. Bässler, A. Ausmees, M. Jurvansuu, R. Feifel, J.-O. Forsell, P. de Tarso Fonseca, A. Kivimäki, S. Sundin, S. L. Sorensen, R. Nyholm, O. Björneholm, S. Aksela, and S. Svensson. Beam line I411 at MAX II - performance and first results. Nucl. Instr. Meth. Phys. Res. A, 469:382–393, 2001.

[38] N. Berrah, B. Langer, A. A. Wills, E. Kukk, J. D. Bozek, A. Farhat, and T. W. Gorczyca. High-resolution angle-resolved measurements in atoms and molecules using advanced photoelectron spectroscopy at the ALS. J. Electron Spectrosc. Relat. Phenom., 101-103:1–11, 1999.

[39] J. Söderström, N. Mårtensson, O. Travnikova, M. Patanen, C. Miron, L. J. Sæthre, K. J. Børve, J. J. Rehr, J. J. Kas, F. D. Vila, T. D. Thomas, and S. Svensson. Nonstoichiometric intensities in core photoelectron spectroscopy. Phys. Rev. Lett., 108:193005–1–4, 2012.

[40] Bastian Holst. Commons. http://commons.wikimedia.org/wiki/File:Undulator.png, 2006. [Online; accessed 14-July-2011].

[41] V. Myrseth, J. D. Bozek, E. Kukk, L. J. Sæthre, and T. D. Thomas. Adiabatic and vertical carbon 1s ionization energies in representative small molecules. J. Electron Spectrosc. Relat. Phenom., 122:57–63, 2002.

[42] R. Nyholm, J. N. Andersen, U. Johansson, B. N. Jensen, and I. Lindau. Beamline I311 at MAX-lab: A VUV/soft X-ray undulator beamline for High Resolution Electron Spectroscopy. Nucl. Instr. and Meth. in Phys. Res. A, 467-468:520–524, 2001.

[43] M. J. Frisch, G. W. Trucks, H. B. Schlegel, G. E. Scuseria, M. A. Robb, J. R. Cheeseman, G. Scalmani, V. Barone, B. Mennucci, G. A. Petersson, H. Nakatsuji, M. Caricato, X. Li, H. P. Hratchian, A. F. Izmaylov, J. Bloino, G. Zheng, J. L. Sonnenberg, M. Hada, M. Ehara, K. Toyota, R. Fukuda, J. Hasegawa, M. Ishida, T. Nakajima, Y. Honda, O. Kitao, H. Nakai, T. Vreven, J. A. Montgomery, Jr., J. E. Peralta, F. Ogliaro, M. Bearpark, J. J. Heyd, E. Brothers, K. N. Kudin, V. N. Staroverov, R. Kobayashi, J. Normand, K. Raghavachari, A. Rendell, J. C. Burant, S. S. Iyengar, J. Tomasi, M. Cossi, N. Rega, J. M. Millam, M. Klene, J. E. Knox, J. B. Cross, V. Bakken, C. Adamo, J. Jaramillo, R. Gomperts, R. E. Stratmann, O. Yazyev, A. J. Austin, R. Cammi, C. Pomelli, J. W. Ochterski, R. L. Martin, K. Morokuma, V. G. Zakrzewski, G. A. Voth, P. Salvador, J. J. Dannenberg, S. Dapprich, A. D. Daniels, O. Farkas, J. B. Foresman, J. V. Ortiz, J. Cioslowski, and D. J. Fox. Gaussian 09 Revision B.01. Gaussian Inc. Wallingford CT 2009.

[44] P. O. Löwdin. Quantum theory of many-particle systems. III. Extension of the Hartree-Fock scheme to include degenerate systems and correlation effects. Phys. Rev., 97:1509–1520, 1955.

[45] W. Koch and M. C. Holthausen. A Chemist's Guide to Density Functional Theory, 2nd ed. Wiley-VCH, Weinheim, 2001.

[46] C. Møller and M. S. Plesset. Note on an approximation treatment for many-electron systems. Phys. Rev., 46:618–622, 1934.

[47] M. Head-Gordon, J. A. Pople, and M. J. Frisch. MP2 energy evaluation by direct methods. Chem. phys. lett., 153:503–506, 1988.

[48] J. A. Pople, M. Head-Gordon, and K. Raghavachari. Quadratic configuration interaction. A general technique for determining electron correlation energies. J. Chem. Phys., 87:5968–5975, 1987.

[49] A. D. Becke. Density-functional thermochemistry. III. The role of exact exchange. J. Chem. Phys., 98:5648–5652, 1993.

[50] C. Lee, W. Yang, and R. G. Parr. Development of the Colle-Salvetti correlation-energy formula into a functional of the electron density. Phys. Rev. B, 37:785–789, 1988.

[51] S. H. Vosko, L. Wilk, and M. Nusair. Accurate spin-dependent electron liquid correlation energies for local spin density calculations: A critical analysis. Can. J. Phys., 58:1200–1211, 1980.

[52] R. Krishnan, J. S. Binkley, R. Seeger, and J. A. Pople. Self-consistent molecular orbital methods. XX. A basis set for correlated wave functions. J. Chem. Phys., 72:650–654, 1980.

[53] C. W. Bauschlicher, A. Ricca Jr., H. Partridge, and S. R. Langhoff. Recent Advances in Density Functional Methods Part II. World Scientific, 1997.

[54] T. H. Dunning, Jr. Gaussian basis functions for use in molecular calculations. III. Contraction of (10s6p) atomic basis sets for the first row atoms. J. Chem. Phys., 55:716–723, 1971.

[55] A. D. McLean and G. S. Chandler. Contracted Gaussian basis sets for molecular calculations. I. Second row atoms, Z=11-18. J. Chem. Phys., 72:5639–5648, 1980.

[56] M. M. Francl, W. J. Pietro, W. J. Hehre, J. S. Binkley, M. S. Gordon, D. J. DeFrees, and J. A. Pople. Self-consistent molecular orbital methods. XXIII. A polarization-type basis set for second-row elements. J. Chem. Phys., 77:3654–3665, 1982.

[57] M. J. Frisch, J. A. Pople, and J. S. Binkley. Self-consistent molecular orbital methods 25. Supplementary functions for Gaussian basis sets. J. Chem. Phys., 80:3265–3269, 1984.

[58] T. H. Dunning Jr. Gaussian basis sets for use in correlated molecular calculations. I. The atoms boron through neon and hydrogen. J. Chem. Phys., 90:1007–1023, 1989.

[59] T. H. Dunning, K. A. Peterson, and A. K. Wilson. Gaussian basis sets for use in correlated molecular calculations. X. The atoms aluminum through argon revisited. J. Chem. Phys., 114:9244–9253, 2001.

[60] W. J. Stevens, H. Basch, and M. Krauss. Compact effective potentials and efficient shared-exponent basis sets for the first- and second-row atoms. J. Chem. Phys., 81:6026–6033, 1984.

[61] T. Karlsen and K. J. Børve. Accurate and approximate calculations of Franck-Condon intensities in the carbon 1s photoelectron spectrum of methane. J. Chem. Phys., 112:7979–7985, 2000.

[62] K. Aidas, C. Angeli, K. L. Bak, V. Bakken, R. Bast, L. Boman, O. Christiansen, R. Cimiraglia, S. Coriani, P. Dahle, E. K. Dalskov, U. Ekström, T. Enevoldsen, J. J. Eriksen, P. Ettenhuber, B. Fernández, L. Ferrighi, H. Fliegl, L. Frediani, K. Hald, A. Halkier, C. Hättig, H. Heiberg, T. Helgaker, A. C. Hennum, H. Hettema, E. Hjertenæs, S. Høst, I.-M. Høyvik, M. F. Iozzi, B. Jansík, H. J. Aa. Jensen, D. Jonsson, P. Jørgensen, J. Kauczor, S. Kirpekar, T. Kjærgaard, W. Klopper, S. Knecht, R. Kobayashi, H. Koch, J. Kongsted, A. Krapp, K. Kristensen, A. Ligabue, O. B. Lutnæs, J. I. Melo, K. V. Mikkelsen, R. H. Myhre, C. Neiss, C. B. Nielsen, P. Norman, J. Olsen, J. M. H. Olsen, A. Osted, M. J. Packer, F. Pawlowski, T. B. Pedersen, P. F. Provasi, S. Reine, Z. Rinkevicius, T. A. Ruden, K. Ruud, V. V. Rybkin, P. Sałek, C. C. M. Samson, A. Sanchez de Meras, T. Saue, S. P. A. Sauer, B. Schimmelpfennig, K. Sneskov, A. H. Steindal, K. O. Sylvester-Hvid, P. R. Taylor, A. M. Teale, E. I. Tellgren, D. P. Tew, A. J. Thorvaldsen, L. Thøgersen, O. Vahtras, M. A. Watson, D. J. D. Wilson, M. Ziolkowski, and H. Ågren. The Dalton quantum chemistry program system. Wiley Interdisciplinary Reviews: Computational Molecular Science, 4:269–284, 2014.

[63] F. B. van Duijneveldt, J. G. C. M. van Duijneveldt-van de Rijdt, and J. H. van Lenthe. State of the art in counterpoise theory. Chem. Rev., 94:1873–1885, 1994.

[64] K. J. Børve and T. D. Thomas. The calculation of initial-state effects on inner-shell ionization energies. J. Electron Spectrosc. Relat. Phenom., 107:155–161, 2000.

[65] L. A. Curtiss, P. C. Redfern, and K. Raghavachari. Gaussian-4 theory. J. Chem. Phys., 126:084108, 2007.

[66] J. Tomasi, B. Mennucci, and R. Cammi. Quantum mechanical continuum solvation models. Chem. Rev., 105:2999–3093, 2005.

[67] L. Hedberg and I. M. Mills. ASYM20 - a program for force-constant and normal-coordinate calculations, with a critical-review of the theory involved. J. Molec. Spectrosc., 160:117–142, 1993.

[68] E. Kukk. Spectral analysis by curve fitting macro package/SPANCF, 2011. URL `http://www.physics.utu.fi/en/research/material_science/Fitting.html`.

[69] WaveMetrics. IGOR Pro 6. URL `http://www.wavemetrics.com`.

[70] P. van der Straten, R. Morgenstern, and A. Niehaus. Angular dependent post-collision interaction in Auger processes. Z. Phys. D, 8:35–45, 1988.

[71] T. X. Carroll, N. Berrah, J. Bozek, J. Hahne, E. Kukk, L. J. Sæthre, and T. D. Thomas. Carbon 1s photoelectron spectrum of methane: Vibrational excitation and core-hole lifetime. Phys. Rev. A, 59:3386–3393, 1999.

[72] T. X. Carroll, J. A. Hahne, T. D. Thomas, L. J. Sæthre, N. Berrah, J. D. Bozek, and E. Kukk. Carbon 1s core-hole lifetime in CO_2. Phys. Rev. A, 61:042503–1–7, 2000.

[73] T. D. Thomas, L. J. Sæthre, K. J. Børve, J. D. Bozek, M. Huttula, and E. Kukk. Carbon 1s photoelectron spectroscopy of halomethanes. Effects of electronegativity, hardness, charge distribution, and relaxation. J. Phys. Chem. A, 108:4983–4990, 2004.

[74] IUPAC. Compendium of Chemical Terminology, 2nd ed. (the "Gold Book"). Compiled by A. D. McNaught and A. Wilkinson. Blackwell Scientific Publications, Oxford (1997). XML on-line corrected version: http://goldbook.iupac.org (2006-) created by M. Nic, J. Jirat, B. Kosata; updates compiled by A. Jenkins. ISBN 0-9678550-9-8. doi:10.1351/goldbook. Last update: 2014-02-24; version: 2.3.3.

[75] E. P. L. Hunter and S. G. Lias. Evaluated gas-phase basicities and proton affinties of molecules: An update. J. Phys. Chem. Ref. Data, 27:413–656, 1998.

[76] M. V. Frash, A. C. Hopkinson, and D. K. Bohme. A quantum-chemical study of the $C_2H_3F_2^+$ and $C_2H_3Cl_2^+$ isomers and their interconversion. CBS-QB3 proton affinities of difluoroethenes and dichloroethenes. J. Phys. Chem. A, 103:7872–7882, 1999.

[77] A. Brooks, K.-C. Lau, C.-Y. Ng, and T. Baer. The $C_3H_7^+$ appearance energy from 2-iodopropane and 2-chloropropane studied by threshold photoelectron photoion coincidence. European Journal of Mass Spectrometry, 10(6):819–828, 2004.

[78] B J Smith and L Radom. Heat of formation of the tert-butyl radical. J. Phys. Chem. A, 102:10787–10790, 1998.

[79] Larry A Curtiss, Krishnan Raghavachari, Paul C Redfern, and John A Pople. Assessment of Gaussian-3 and density functional theories for a larger experimental test set. J. Chem. Phys., 112:7374–7383, 2000.

[80] J. McMurry. Organic Chemistry, 8th ed. Cengage Learning, 2012, 2008.

[81] M. A. Turpin, K. C. Smith, G. L. Heard, D. W. Setser, and B. E. Holmes. Unimolecular reactions of 1, 1, 1-trichloroethane, 1, 1, 1-trichloropropane and 3, 3, 3-trifluoro-1, 1, 1-trichloropropane: Deter-

mination of threshold energies by chemical activation. J. Phys. Chem. A, pages 9347–9356, 2014.

[82] Y.-L. Ding, J.-R. Mu, C.-H. Wang, and Z.-Z. Yang. Insight into Markovnikov regioselectivity rule via molecular face and ABEEM $\sigma\pi$ theory. Int. J. Quantum Chem., 111:2778–2787, 2011.

[83] Z.-Z. Yang, Y.-L. Ding, and D. X. Zhao. Insight into Markovnikov reactions of alkenes in terms of ab initio and molecular face theory. ChemPhysChem, 9:2379–2389, 2008.

[84] A. Holme, K. J. Børve, L. J. Sæthre, and T. D. Thomas. Accuracy of calculated chemical shifts in carbon 1s ionization energies from single-reference *ab initio* methods and density functional theory. J. Chem. Theory Comput., 7:4104–4114, 2011.

[85] J. H. Callomon, E. Hirota, K. Kuchitsu, W. J. Lafferty, A. G. Maki, and C. S. Pote. Group II: Atomic and molecular physics. Volume 7: Structure data of free polyatomic molecules. In K.-H. Hellwege and A. M. Hellwege, editors, Landolt-Börnstein: Numerical Data and Functional Relationships in Science and Technology, New Series. Springer-Verlag Berlin, Heidelberg, New York, 1976.

[86] T. R. Walsh, T. E. Meehan, and F. P. Larkins. Prediction of molecular Auger rates using a statistical model. J. Phys. B: At. Mol. Opt. Phys., 27:2211–2216, 1994.

[87] R. W. Shaw Jr and T. D. Thomas. Chemical effects on the lifetime of 1 s-hole states. Phys. Rev. Lett., 29:689, 1972.

[88] S. H. Schei and Q. Shen. 3-Chloro-1-propene (allylchloride): Gas-phase molecular structure and conformations as determined by electron diffraction. J. Mol. Struct., 128:161–170, 1985.

[89] M. Abu-Samha, K. J. Børve, L. J. Sæthre, and T. D. Thomas. Conformational effects in inner-shell photoelectron spectroscopy of ethanol. Phys. Rev. Lett., 95:103002–1–4, 2005.

[90] A. Holme, L. J. Sæthre, K. J.Børve, and T. D. Thomas. J. Mol. Struct., 920:387–392, 2009.

[91] Z. He, X. Yang, X. J. Zhou, and K. T. Leung. Room-temperature chemisorption of chloroethylenes on Si(111)7×7: formation of surface vinyl, vinylidene and their chlorinated derivatives. Surf. Sci., 547:L840–L846, 2003.

[92] Z. He, Q. Li, and K. T. Leung. Room-temperature chemisorption and thermal evolution of 1,1-dichloroethylene and monochloroethylene on

Si(111)7×7: formation of vinylidene and vinylene adspecies. J. Phys. Chem. B, 109:14908–14916, 2005.

[93] Z. He, Q. Li, and K. T. Leung. Isomeric effects on room-temperature chemisorption and thermal evolution of *iso*-, *cis*- and *trans*-dichloroethylene on Si(111)7×7. Surf. Sci., 600:514–526, 2006.